molecules

MDPI

Article

Metabolites of Medicarpin and Their Distributions in Rats

Hong-Yan Wang [1], Teng Li [1], Rui Ji [1,2], Feng Xu [1,*], Guang-Xue Liu [1], Yao-Li Li [1], Ming-Ying Shang [1,*] and Shao-Qing Cai [1]

[1] State Key Laboratory of Natural and Biomimetic Drugs, School of Pharmaceutical Sciences, Peking University, No. 38, Xueyuan Road, Beijing 100191, China; wanghongyan@bjmu.edu.cn (H.-Y.W.); tengli1175@163.com (T.L.); jiruiwonder@163.com (R.J.); guangxl@bjmu.edu.cn (G.-X.L.); liyaoli123456@163.com (Y.-L.L.); sqcai@bjmu.edu.cn (S.-Q.C.)

[2] School of Pharmacy, Heilongjiang University of Chinese Medicine, No.24, Heping Road, Xiangfang District, Harbin 150040, China

* Correspondence: xufeng76@bjmu.edu.cn (F.X.); myshang@bjmu.edu.cn (M.-Y.S.); Tel.: +86-10-8280-2534 (F.X. & M.-Y.S.)

Received: 22 April 2019; Accepted: 18 May 2019; Published: 22 May 2019

Abstract: Medicarpin is a bioactive pterocarpan that has been attracting increasing attention in recent years. However, its metabolic fate in vivo is still unknown. To clarify its metabolism and the distribution of its metabolites in rats after oral administration, the HPLC-ESI-IT-TOF-MS^n technique was used. A total of 165 new metabolites (13 phase I and 152 phase II metabolites) were tentatively identified, and 104, 29, 38, 41, 74, 28, 24, 15, 42, 8, 10, 3, and 17 metabolites were identified in urine, feces, plasma, the colon, intestine, stomach, liver, spleen, kidney, lung, heart, brain, and thymus, respectively. Metabolic reactions included demethylation, hydrogenation, hydroxylation, glucuronidation, sulfation, methylation, glycosylation, and vitamin C conjugation. **M1** (medicarpin glucuronide), **M5** (vestitol-1′-*O*-glucuronide) were distributed to 10 organs, and **M1** was the most abundant metabolite in seven organs. Moreover, we found that isomerization of medicarpin must occur in vivo. At least 93 metabolites were regarded as potential new compounds by retrieving information from the Scifinder database. This is the first detailed report on the metabolism of ptercarpans in animals, which will help to deepen the understanding of the metabolism characteristics of medicarpin in vivo and provide a solid basis for further studies on the metabolism of other pterocarpans in animals.

Keywords: medicarpin; pterocarpan; metabolites; distribution; in vivo; HPLC-ESI-IT-TOF-MS^n

1. Introduction

Pterocarpans are the second largest group of dihydroisoflavonoids and have a special structure skeleton (benzopyran-benzofuran four-ring system). They were originally isolated from plants [1] and then regarded as an important group of phytoalexins, which have antifungal [2] and antibacterial [3] effects. In recent years, many new bioactivities of pterocarpans have been discovered, such as anti-inflammation [4–6], antitumor activity [7–9], anti-osteoporosis [10–12], antimalarial [13], antioxidant [14–16], inhibition of neuraminidase [17–19] and melanin synthesis [20], estrogenic and anti-estrogenic activity [21], anti-clastogensis [22], immunosuppressive activity [23], and inhibition of acetylcholinesterase [24]. As a result, this group of natural products is getting more and more attention. However, after conducting a systematic literature survey, we surprisingly found that there is only one report on the metabolism of a pure pterocarpan (i.e., trifolirhizin) in animals and only two metabolites (maackiain in feces and maackiain, maackiain-3-*O*-sulfoacid in urine) were identified [25], though a lot

of papers about biosynthesis and the fungal metabolism of pterocarpans have been published. Drug metabolism research has a pivotal role in new drug research and development. In order to effectively utilize pterocarpans, it is important to clarify their metabolism characteristics.

Medicarpin (Figure 1) is a natural pterocarpan-type phytoalexin [26] with a wide variety of biological activities distributed in lots of traditional Chinese medicines (TCM), such as Pueraria Lobata [27], and Hedysari Radix [28]. According to the literature, medicarpin has anti-osteoporotic and bone protection activities even at a low concentration of 10^{-4} μM on murine bone cells and it can reduce the formation of osteoclasts but increase the formation of osteoprogenitor cells in bone marrow cells (BMCs) in OVx mice at a dose of 10 mg/kg/d for 30 days [10]. In another study, medicarpin treatment (10 mg/kg/d for 30 days) can increase the formation of osteoprogenitor cells in BMCs and osteoid formation in female Sprague-Dawley (SD) rats [11]. It also shows cytotoxic activities in BCA-1 (human breast cancer cells, IC_{50} = 13.14 μg/mL) and KB (human epidermoid carcinoma of cavity, IC_{50} = 10.13 μg/mL) cells [29]. In addition, medicarpin can lead to apoptosis and reverse multidrug resistance in P388 leukemia cells (IC_{50} ≈ 90 μM) [30]. It also has antifungal [31] and antibacterial activities [32]. Additionally, medicarpin can stimulate mesenchymal stem cells to differentiate into brown and beige adipocytes via the adenosine monophosphate-activated protein kinase (AMPK) pathway and boost lipolysis in adipocytes via a protein kinase A (PKA)-dependent pathway, so it is expected to be a potential drug for the treatment of obesity [33,34]. However, the metabolism of medicarpin in vivo and in vitro is still unknown. Therefore, the present study aims to identify its metabolites, clarify its metabolic pathways, and reveal the distribution of medicarpin and its metabolites in rats using high-performance liquid chromatography-electrospray ionization-ion trap-time of flight-multistage mass spectrometry (HPLC-ESI-IT-TOF-MS^n).

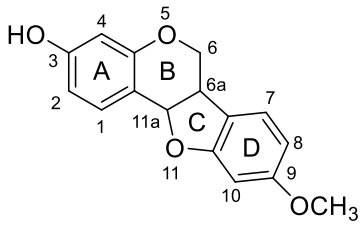

Figure 1. The structure and atom numbering of medicarpin.

2. Results and Discussion

2.1. MS Fragmentation Characteristics of Medicarpin in ESI− Mode and Identification of Medicarpin in Rats

In order to facilitate the description of the ESI− MS characteristics of medicarpin and its metabolites, we proposed a nomenclature for the fragmentation pathways and fragment ions. The four rings were named A, B, C and D, respectively. The cleavable C-C bonds in the skeleton were designated by numbers 1–8, as shown in Figure 2.

Medicarpin ($C_{16}H_{14}O_4$) showed $[M - H]^-$ at *m*/*z* 269.0822 (theoretical mass was 269.0819 Da) in ESI− spectra. The characteristic fragment ions of medicarpin in ESI− mode included *m*/*z* 254.0586 ($[M - H - CH_3\bullet]^{\bullet-}$), *m*/*z* 161.0173 ($C_9H_5O_3$, $^{6,8}A^- - 2H$), *m*/*z* 145.0387 ($C_9H_5O_2$, $^{6,7}A^- - 2H$), *m*/*z* 133.0302 ($C_8H_5O_2$, $^{3,4,7}A^- - H$), *m*/*z* 132.0270 ($C_8H_4O_2$, $^{3,5}D^- - CH_3\bullet$), *m*/*z* 121.0358 ($C_7H_5O_2$, $^{3,5}A^-$) in its MS^2 spectra (Figure 2).

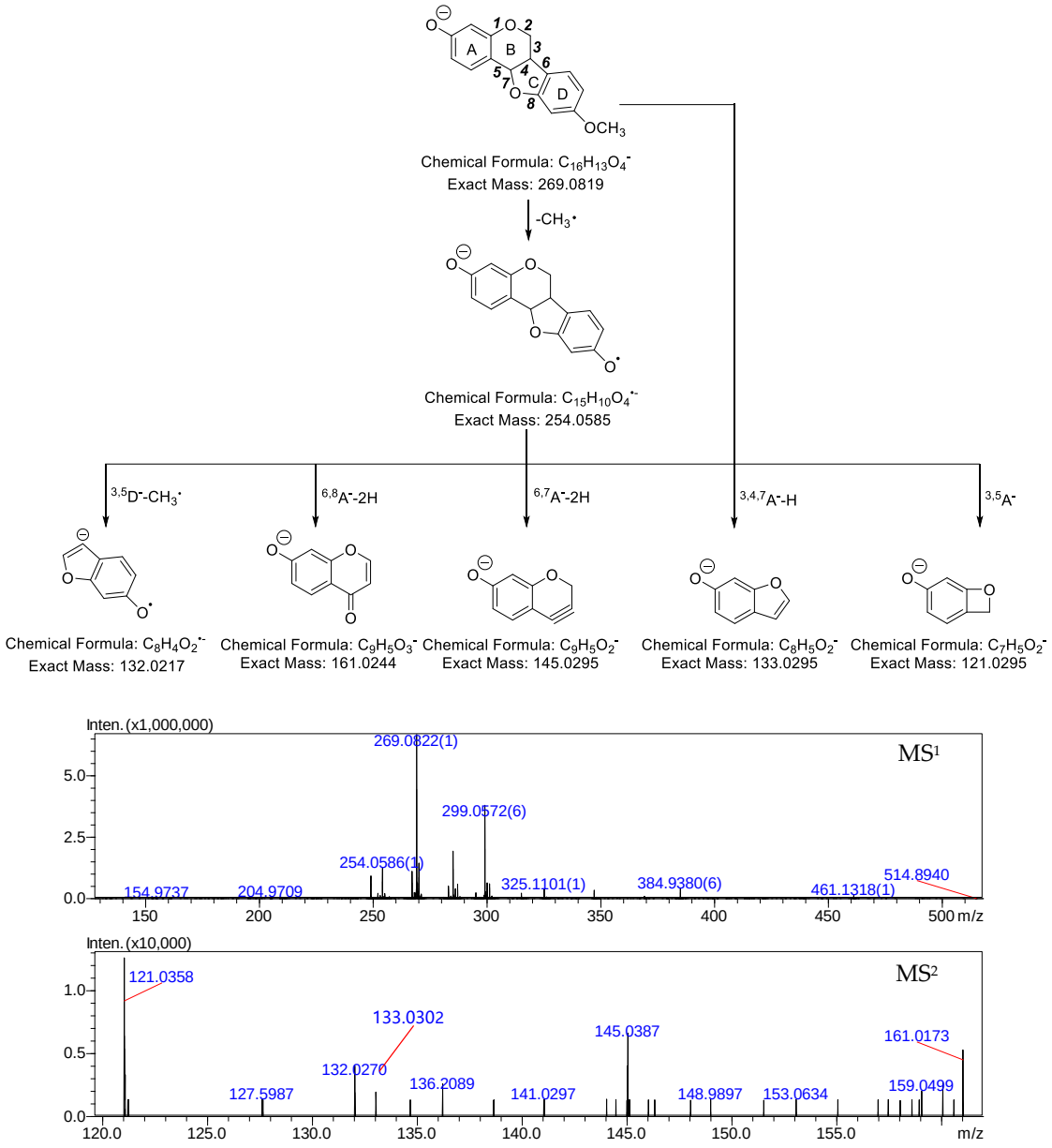

Figure 2. The MS spectra and the proposed fragmentation pathways of medicarpin in ESI− mode.

2.2. *Profiling 165 Metabolites of Medicarpin in Rats*

The metabolites of medicarpin were screened by comparing the HPLC chromatograms and MS base peak chromatograms (BPCs) of drug and blank group samples obtained through HPLC-ESI-IT-TOF-MS^n analysis, and then confirmed by comparison of extracted ion chromatograms (EICs) between the drug and blank groups. The metabolic reactions were judged by the accurate mass (elemental composition) differences between medicarpin and its metabolites. The accurate mass (elemental composition) differences of −14.01 Da (CH_2), +14.01 Da (CH_2), +2.01 Da (H_2), and +15.99 Da (O) indicated demethylation, methylation, hydrogenation and hydroxylation. The loss of 176.03 Da ($C_6H_8O_6$) from precursor ion and/or an anion at *m*/*z* 175.02 in MS^2 spectra indicated that the metabolite was a glucuronide; the loss of 79.95 Da (SO_3) from precursor ion indicated that the metabolite was a sulfate; the loss of 162.05 Da ($C_6H_{10}O_5$) indicated a hexoside (more likely to be a glucoside); the loss of 158.02 Da ($C_6H_6O_5$) indicated a vitamin C conjugate [35].

A total of 165 metabolites of medicarpin were confirmed and tentatively identified by the above-mentioned method, and the proposed metabolic pathways of medicarpin are shown in Figure 3.

According to the skeleton of molecules, 165 metabolites were classified into 13 categories: (1) metabolites (**M1**–**M3**) having the skeleton of medicarpin; (2) metabolites (**M4**–**M10**) having the skeleton of hydrogenated medicarpin; (3) metabolites (**M11**–**M26**) having the skeleton of demethylated medicarpin; (4) metabolites (**M27**–**M52**) having the skeleton of demethylated and hydrogenated medicarpin; (5) metabolites (**M53**–**M75**) having the skeleton of demethylated and hydroxylated medicarpin; (6) metabolites (**M76**–**M107**) having the skeleton of hydroxylated medicarpin; (7) metabolites (**M108**–**M138**) having the skeleton of hydrogenated and hydroxylated medicarpin; (8) metabolites (**M139**–**M149**) having the skeleton of demethylated, hydrogenated and hydroxylated medicarpin; (9) metabolites (**M150**–**M156**) having the skeleton of demethylated and dihydroxylated medicarpin; (10) metabolites (**M157**–**M161**) having the skeleton of dihydroxylated medicarpin; (11) metabolite (**M162**) having the skeleton of hydrogenated and dihydroxylated medicarpin; (12) metabolites (**M163**–**M164**) having the skeleton of hydrogenated and trihydroxylated medicarpin; (13) metabolite (**M165**) having the skeleton of demethylated, hydrogenated and dihydroxylated medicarpin. The EICs of 165 metabolites are shown in Figures S1–S44.

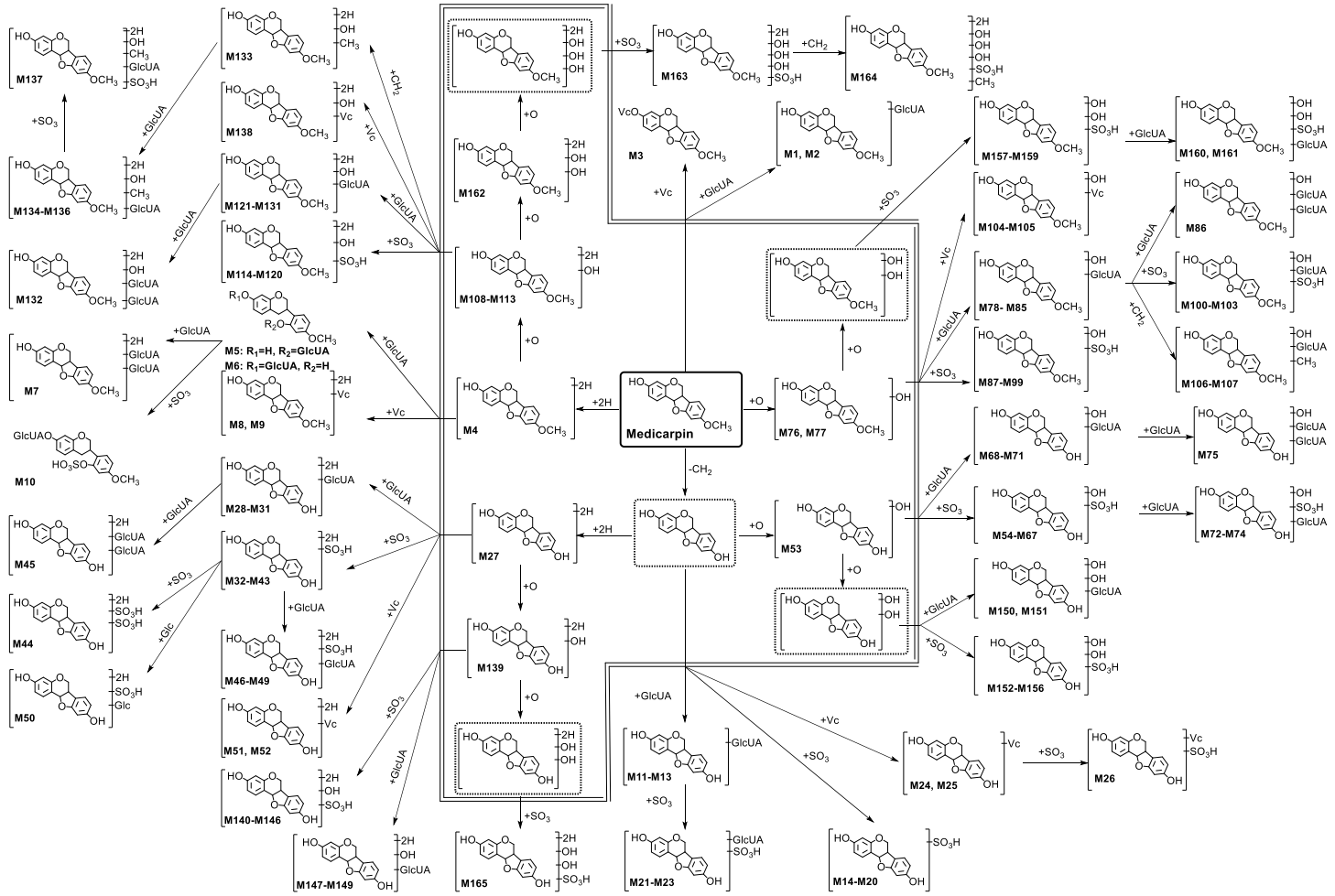

Figure 3. The proposed metabolic pathways of medicarpin in rats. Phase I metabolites are in the double line polygon, undetected intermediates are in the dashed line boxes.

2.2.1. Analysis of Metabolites (**M1**–**M3**) Having the Skeleton of Medicarpin

M1 and **M2** showed $[M - H]^-$ at *m*/*z* 445.11 and their molecular formulae were predicted to be $C_{22}H_{22}O_{10}$, so they were isomers. The fragment ions at *m*/*z* 269.08 and *m*/*z* 175.02 can be detected in both of their MS^2 spectra. Therefore, **M1** and **M2** were determined to be glucuronides of medicarpin. However, medicarpin only has one hydroxyl group, i.e., one glucuronidation site (Figure 4a). Hence, we deduced that isomerization of medicarpin (configuration change or shift of substituent) must occur.

M3 (Figure 5) showed $[M - H]^-$ at *m*/*z* 427.1049 and its molecular formula was predicted to be $C_{22}H_{20}O_9$. In its MS^2 spectra, *m*/*z* 269.0792 ($C_{16}H_{13}O_4$, [medicarpin − H]$^-$) formed by losing 158.02 Da ($C_6H_6O_5$) from $[M - H]^-$ was observed, indicating a vitamin C conjugate based on our previous study [35]. Besides, in the ESI+ mode, **M3** showed $[M + H]^+$ at *m*/*z* 429.1177. In its MS^2 spectra, fragment ion at *m*/*z* 313.1113 was observed, indicating a neutral loss of 116.01 Da ($C_4H_4O_4$). Subsequently, *m*/*z* 313.1113 yielded fragment ions at *m*/*z* 165.0516 ($C_9H_9O_3$), *m*/*z* 161.0577 ($C_{10}H_9O_2$) and *m*/*z* 137.0600 ($C_8H_9O_2$). Hence, **M3** was medicarpin-3-*O*-vitamin C.

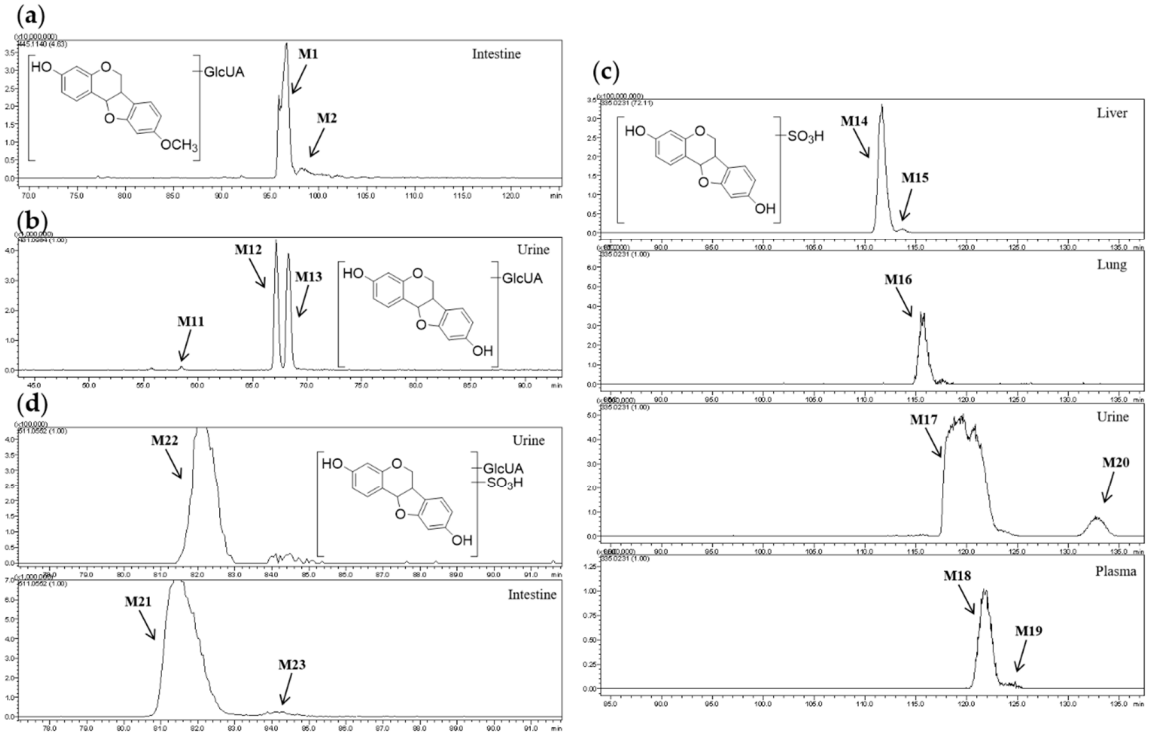

Figure 4. (**a**) Extracted ion chromatograms (EIC) of *m*/*z* 445.11; (**b**) EIC of *m*/*z* 431.10; (**c**) EIC of *m*/*z* 335.02; (**d**) EIC of *m*/*z* 511.06.

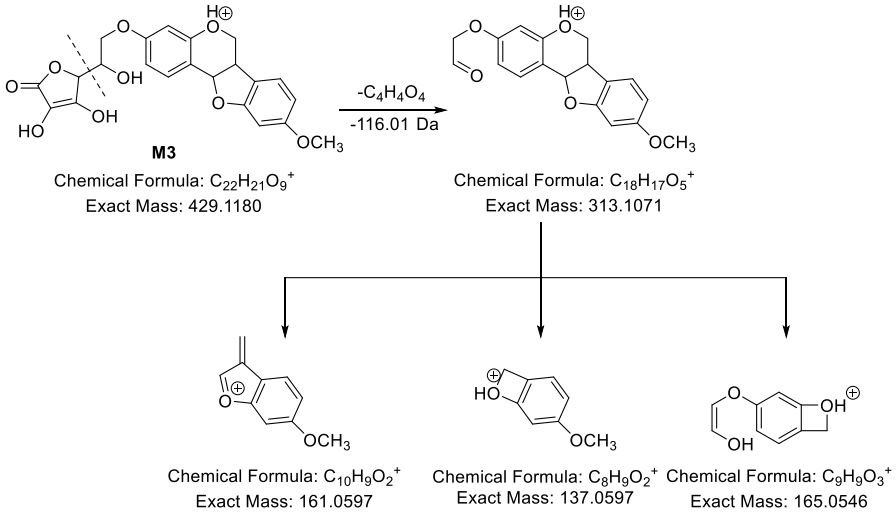

Figure 5. The proposed fragmentation pathways of **M3** in ESI+ mode.

2.2.2. Analysis of Metabolites (**M4**–**M10**) Having the Skeleton of Hydrogenated Medicarpin

M4 showed $[M - H]^-$ at *m*/*z* 271.0979, and its molecular formula was predicted to be $C_{16}H_{16}O_4$, which had two more hydrogen atoms than that of medicarpin. Therefore, one ring of medicarpin must be cleaved. In its MS^2 spectra, the fragment ions at *m*/*z* 147.0469 ($C_9H_7O_2$, $^6A^-$ or $^{3,5}B^-$ − 2H), *m*/*z* 135.0466 ($C_8H_7O_2$, $^{3,4}A^-$ or $^{3,4}B^-$), *m*/*z* 123.0543 ($C_7H_7O_2$, $^6B^-$ + H or $^{3,5}A^-$ + 2H or $^{2,4}A^-$ + 2H), *m*/*z* 121.0302 ($C_7H_5O_2$, $^{3,5}A^-$ or $^{2,4}A^-$) and *m*/*z* 109.0321 ($C_6H_5O_2$, $^{2,5}A^-$ + 2H) were detected. According to the characteristic fragment ion at *m*/*z* 135.0466 ($C_8H_7O_2$, $^{3,4}A^-$ or $^{3,4}B^-$), we could deduce that medicarpin had undergone ring cleavage at the bond of C11-C11a as shown in Figure 6a. Hence, **M4** was determined to be vestitol. The characteristic fragment ion at *m*/*z* 135.05 ($C_8H_7O_2$) was very useful, because its existence indicated that the C11-C11a bond was cleaved and the hydrogenated medicarpin had the skeleton of a vestitol. The MS^2 spectrum of **M4** is shown in Figure S45.

M5 and **M6** showed $[M - H]^-$ at *m*/*z* 447.13, and their molecular formulae were predicted to be $C_{22}H_{24}O_{10}$. Moreover, the fragment ions at *m*/*z* 271.09, *m*/*z* 175.02, *m*/*z* 147.05 ($C_9H_7O_2$, $^6A^-$ or $^{3,5}B^-$ − 2H) and *m*/*z* 135.05 ($C_8H_7O_2$, $^{3,4}A^-$ or $^{3,4}B^-$) could be detected in their MS^2 spectra. Based on *m*/*z* 135.05 ($C_8H_7O_2$), we could deduce that the ring-cleavage took place at the bond of C11-C11a. Because a larger CLogP value means a lower polarity and a larger retention time in reversed phase HPLC, so **M5** (CLogP = 0.7229, t_R = 90.033) was assigned as vestitol-1′-*O*-glucuronide and **M6** (CLogP = 0.9229, t_R = 92.050) was vestitol-7-*O*-glucuronide.

M8 and **M9** showed $[M - H]^-$ at *m*/*z* 429.12 and their molecular formulae were predicted to be $C_{22}H_{22}O_9$, and they yielded a fragment ion at *m*/*z* 271.09 by neutral loss of 158.02 Da ($C_6H_6O_5$). In their MS^3 spectra, the characteristic fragment ions at *m*/*z* 147.05 ($C_9H_7O_2$, $^6A^-$ or $^{3,5}B^-$ − 2H), *m*/*z* 135.05 ($C_8H_7O_2$, $^{3,4}A^-$ or $^{3,4}B^-$) and *m*/*z* 109.03 ($C_6H_5O_2$, $^{2,5}A^-$ + 2H) were observed. Thus, **M8** and **M9** were determined as vestitol vitamin C conjugates.

The molecular formula of **M10** (Figure 6b) was calculated as $C_{22}H_{24}O_{13}S$ based on the $[M - H]^-$ at *m*/*z* 527.0883. The fragment ions at *m*/*z* 351.0505 and *m*/*z* 271.0944 were observed in MS^2 spectra and *m*/*z* 147.0546 ($C_9H_7O_2$), *m*/*z* 135.0498 ($C_8H_7O_2$, $^{3,4}A^-$ or $^{3,4}B^-$) and *m*/*z* 121.0354 ($C_7H_5O_2$) were detected in MS^3 spectra. This indicated that **M10** was a hydrogenated medicarpin glucuronide sulfate. Besides, based on *m*/*z* 135.0498 ($C_8H_7O_2$), we could deduce that the bond of C11-C11a in medicarpin was cleaved. Moreover, the fragment ion at *m*/*z* 254.9829 ($C_{10}H_7O_6S$,), which was derived from precursor ion *m*/*z* 527.0901, indicated that the sulfonic group (-SO_3H) was linked to the fragment of $C_{10}H_7O_3$ ($^{1,5}B^-$ − 4H), and the fragment ion at *m*/*z* 229.0156 ($C_9H_9O_5S$), which was obtained from precursor ion *m*/*z* 351.0505, indicated that -SO_3H was linked to the fragment of $C_9H_9O_2$ ($^{3,5}B^-$). Hence, we could deduce that the sulfonic group was linked to the hydroxyl group of B ring, while the glucuronyl

group was linked to the hydroxyl group of A ring. Therefore, **M10** was unambiguously identified as vestitol-7-*O*-glucuronide-1′-*O*-sulfate. The MS spectra of **M10** are shown in Figure S46.

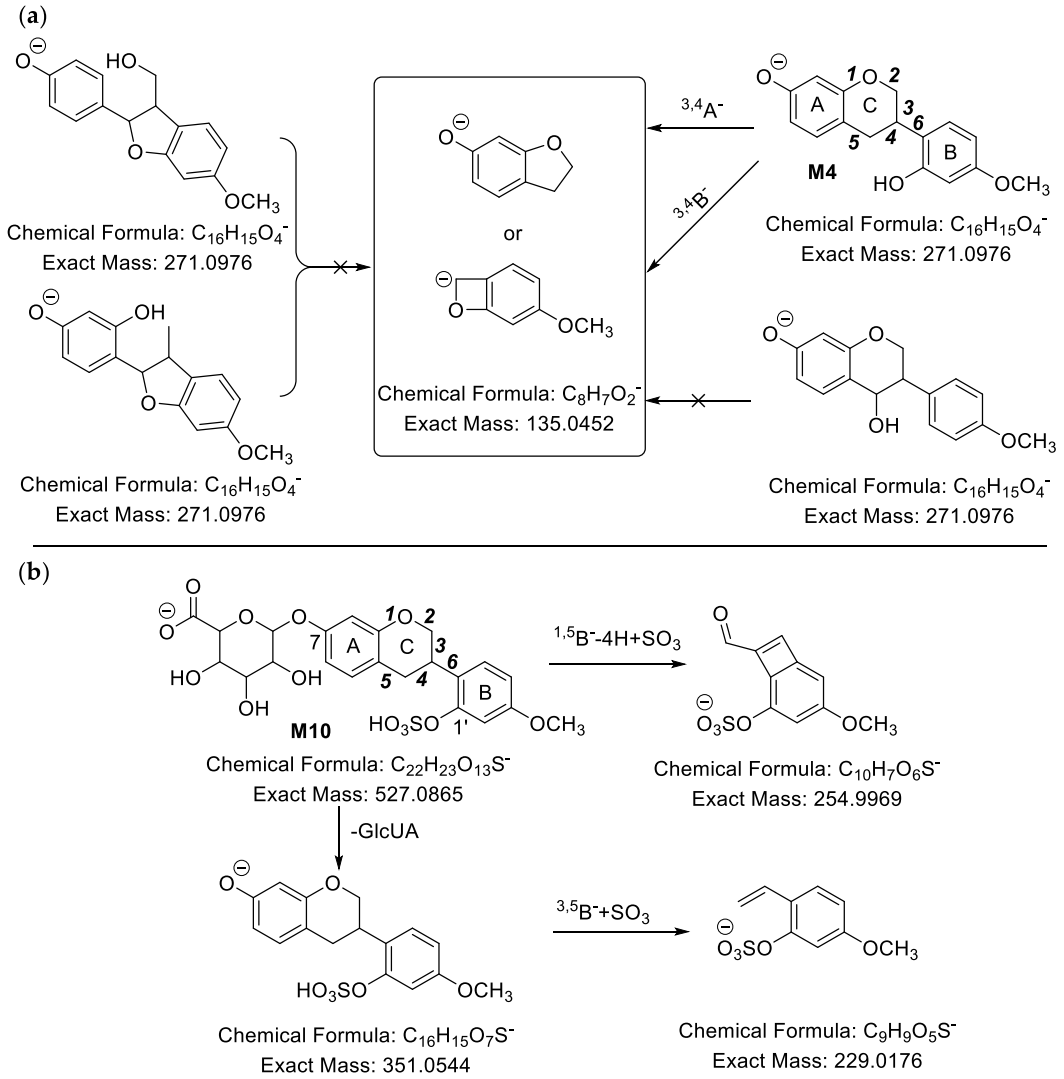

Figure 6. (**a**) The proposed fragmentation pathways of **M4** in ESI− mode; (**b**) The proposed fragmentation pathways of **M10** in ESI− mode.

2.2.3. Analysis of Metabolites (**M11**–**M26**) Having the Skeleton of Demethylated Medicarpin

M11–**M13** (Figure 4b) showed $[M - H]^-$ at *m*/*z* 431.10, and their molecular formulae were predicted to be $C_{21}H_{20}O_{10}$. Compared with $[Aglycon - H]^-$ ($C_{15}H_{11}O_4$) at *m*/*z* 255.07, the neutral loss was 176.03 Da ($C_6H_8O_6$), indicating that **M11**–**M13** were glucuronides of demethylated medicarpin.

M14–**M20** (Figure 4c) were isomers whose molecular formulae were calculated to be $C_{15}H_{12}O_7S$ based on $[M - H]^-$ at *m*/*z* 335.02. According to the neutral loss 79.95 Da (SO_3), we speculated that **M14**–**M20** were sulfates of demethylated medicarpin.

The molecular formulae of **M21**–**M23** (Figure 4d) were predicted to be $C_{21}H_{20}O_{13}S$ based on $[M - H]^-$ at *m*/*z* 511.06. In their MS^2 spectra, fragment ions at *m*/*z* 335.02 and *m*/*z* 255.07 which were formed by sequential neutral losses of 176.03 Da ($C_6H_8O_6$) and 79.95 Da (SO_3) were observed, demonstrating that **M21**–**M23** were demethylated medicarpin glucuronide sulfates.

Demethylated medicarpin only has two metabolism sites (two free hydroxyl groups), but it has three glucuronidation metabolites (**M11**–**M13**), seven sulfation metabolites (**M14**–**M20**) and three

glucuronidation and sulfation metabolites (**M21**–**M23**). Therefore, we can confirm that isomerization of medicarpin (configuration change or shift of substituent) must occur.

2.2.4. Analysis of Metabolites (**M27**–**M52**) Having the Skeleton of Demethylated and Hydrogenated Medicarpin

M27 (Figure 7a) showed $[M - H]^-$ at *m*/*z* 257.0820, and the molecular formula was predicted to be $C_{15}H_{14}O_4$. Compared with $C_{16}H_{14}O_4$ of medicarpin, it has one less carbon atom. In its MS^2 spectra, there were a series of fragment ions at *m*/*z* 149.0289 ($C_8H_5O_3$), *m*/*z* 147.0481 ($C_9H_7O_2$), *m*/*z* 135.0494 ($C_8H_7O_2$), *m*/*z* 121.0329 ($C_7H_5O_2$) and *m*/*z* 109.0263 ($C_6H_5O_2$). Based on the fragment ion at 149.0289 ($C_8H_5O_3$), we could determine that the **M27** might be **O**, **Q** or **R**. **M37** (Figure 7b) presented $[M - H]^-$ at *m*/*z* 337.0392, therefore its molecular formula was calculated to be $C_{15}H_{14}O_7S$. We could speculate that it was the sulfate of demethylated and hydrogenated medicarpin based on the neutral loss of 79.95 Da (SO_3) and fragment ion at *m*/*z* 257.0804 ($[Aglycon - H]^-$). Besides, fragment ions at *m*/*z* 151.0443 ($C_8H_7O_3$), *m*/*z* 147.0456 ($C_9H_7O_2$), *m*/*z* 135.0461 ($C_8H_7O_2$), *m*/*z* 121.0267 ($C_7H_5O_2$), *m*/*z* 119.0586 (C_8H_7O) and *m*/*z* 109.0234 ($C_6H_5O_2$) were observed. Based on fragment ions at *m*/*z* 215.0033 ($C_8H_7O_5S$) and *m*/*z* 196.9928 ($C_8H_5O_4S$), which were yielded from *m*/*z* 215.0033 ($C_8H_7O_5S$) by the loss of 18.01 Da (H_2O), we could deduce that the skeleton of $C_8H_7O_2$ had two hydroxyl groups and the sulfonic group was linked to the B ring. As a result, the aglycon of **M37** must be **Q**. The characteristic fragment ions of **M27** and **M37** are shown in Figure 7. The MS spectrum of **M37** is shown in Figure S47.

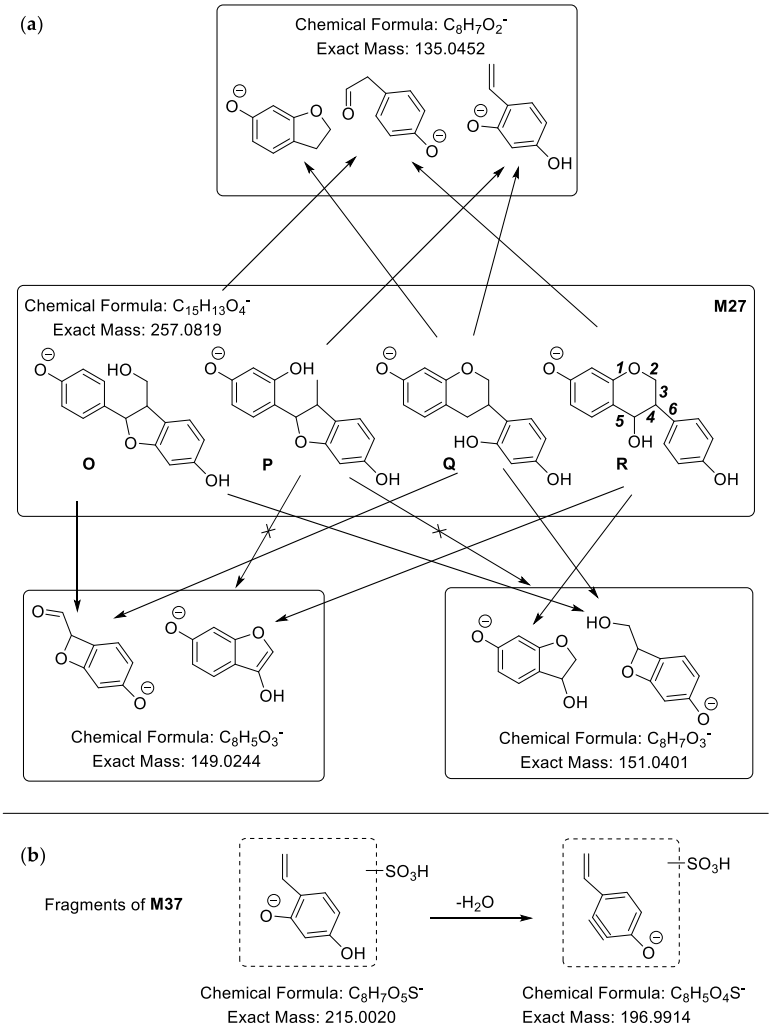

Figure 7. Characteristic fragment ions of **M27** (**a**) and **M37** (**b**) in ESI− mode.

2.2.5. Analysis of Metabolites (**M53**–**M75**) Having the Skeleton of Demethylated and Hydroxylated Medicarpin

M53 presented $[M - H]^-$ at *m/z* 271.0612, and the molecular formula was indicated to be $C_{15}H_{12}O_5$. Compared with $C_{16}H_{14}O_4$ of medicarpin, it has a less CH_2 and one more oxygen atom. Furthermore, according to the fragment ions at *m/z* 161.0281 ($C_9H_5O_3$), *m/z* 149.0273 ($C_8H_6O_3$), *m/z* 137.0283 ($C_7H_5O_3$), *m/z* 133.0249 ($C_8H_5O_2$), *m/z* 121.0406 ($C_7H_5O_2$) and *m/z* 109.0327 ($C_6H_5O_2$), **M53** was determined to be demethylated and hydroxylated medicarpin. However, due to the special structure of the demethylated medicarpin, it is impossible to judge the position of hydroxylation based on the current mass spectrometry data.

2.2.6. Analysis of Metabolites (**M76**–**M107**) Having the Skeleton of Hydroxylated Medicarpin

The molecular formulae of **M87**–**M99** were predicted to be $C_{16}H_{14}O_8S$ due to the pseudomolecular ion peak $[M - H]^-$ at *m/z* 365.04. In their MS^2 spectra, the fragment ion at *m/z* 285.08 ($C_{16}H_{13}O_5$) formed by the loss of 79.95 Da (SO_3) was detected. Therefore, **M87**–**M99** were hydroxylated medicarpin sulfates.

M88 (Figure 8) possessed fragment ions at *m/z* 285.0727, *m/z* 270.0564, *m/z* 161.0254 ($C_9H_5O_3$, $^{6,8}A^- - 2H$ or $^{3,5}B^- - 2H$), *m/z* 139.0337 ($C_7H_7O_3$, $^{6,7}B^- + 2H$) and *m/z* 124.0179 ($C_6H_4O_3$, $^{6,7}B^- + 2H - CH_3\bullet$). Based on the fragment ion at *m/z* 124.0179 ($C_6H_4O_3$, $^{6,7}B^- + 2H - CH_3\bullet$), generated from the fragment ion at *m/z* 270.0564, we deduced that the newly added hydroxyl group was linked to the D ring of **M88**.

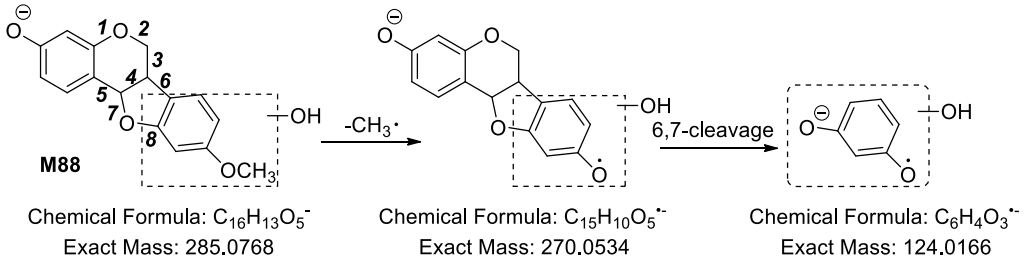

Figure 8. The proposed fragmentation pathways of **M88** in ESI− mode.

2.2.7. Analysis of Metabolites (**M108**–**M138**) Having the Skeleton of Hydrogenated and Hydroxylated Medicarpin

M112 (Figure 9) showed $[M - H]^-$ at *m/z* 287.0943 and the molecular formula was calculated to be $C_{16}H_{16}O_5$, which was two hydrogen atoms and one oxygen atom more than that of medicarpin. Therefore, we speculated that **M112** was hydrogenated and hydroxylated medicarpin. In its MS^2 spectra, a characteristic fragment ion at *m/z* 125.0181 ($C_6H_5O_3$, $^{2,5}A^- + 2H$) was observed, indicating that the newly added hydroxyl group was linked to the A ring, so it has three possibilities **O**, **P** or **Q**. Besides, based on the fragment ion at *m/z* 151.0451 ($C_8H_7O_3$, $^{3,4}A^-$), we could determine that the bond of C11-C11a was cleaved. Finally, the structure of **M112** was determined to be **O**. Furthermore, the fragment ions of **M112** including *m/z* 163.0388 ($C_9H_7O_3$, $^{6}A^- - H$), *m/z* 149.0532 ($C_9H_9O_2$, $^{3,5}B^-$), *m/z* 145.0348 ($C_9H_5O_2$, $^{6}A^- - H - H_2O$), *m/z* 137.0334 ($C_7H_5O_3$, $^{2,4}A^-$ or $^{3,5}A^-$) and *m/z* 134.0482 ($C_8H_6O_2$, $^{3,5}B^- - CH_3\bullet$) supported our elucidation. The MS^2 spectrum of **M112** is shown in Figure S48.

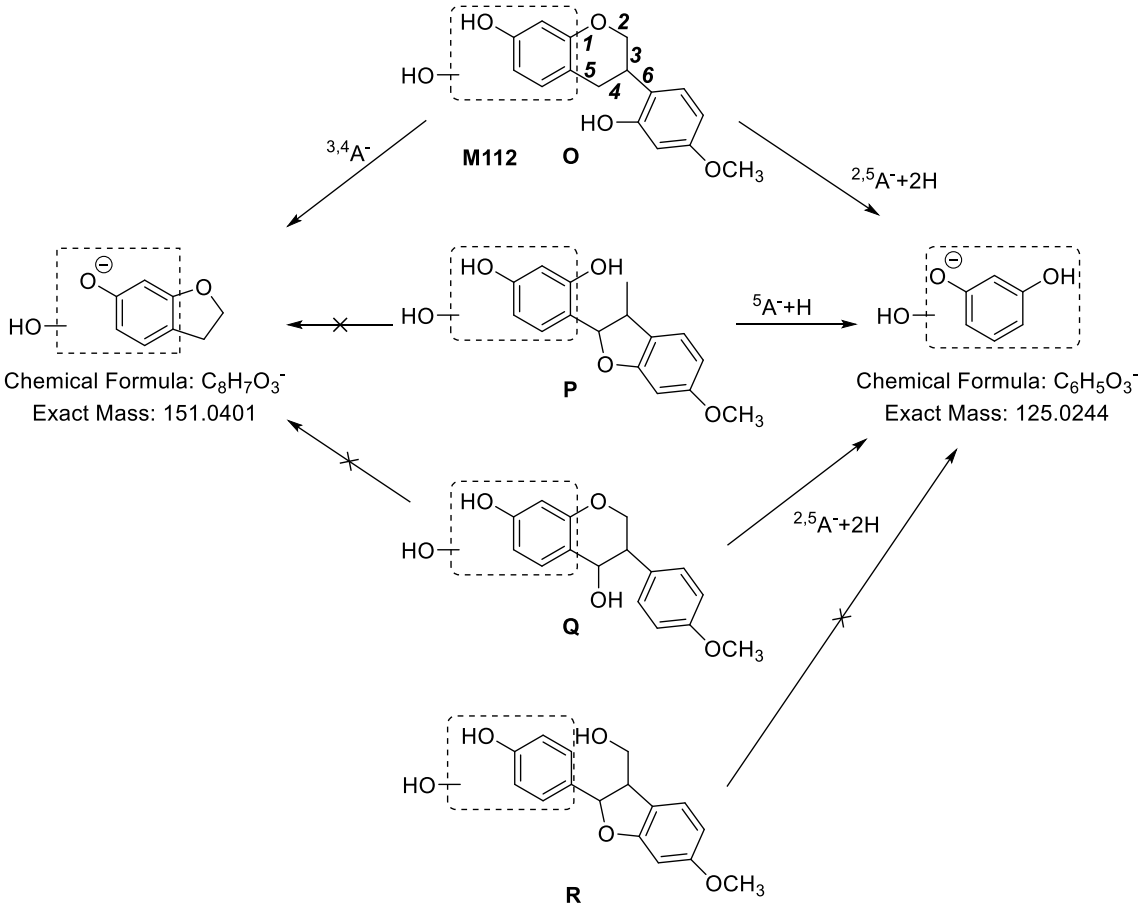

Figure 9. The proposed fragmentation pathways of **M112** in ESI− mode.

The molecular formulae of **M114**–**M120** were predicted as $C_{16}H_{16}O_8S$ based on their $[M - H]^-$ at *m*/*z* 367.05. In their MS^2 spectra, *m*/*z* 287.09 ($C_{16}H_{15}O_5$) was detected, indicating a neutral loss of 79.95 Da (SO_3). Therefore, **M114**–**M120** were determined as hydrogenated and hydroxylated medicarpin sulfates.

M114 (Figure 10) showed fragment ions at *m*/*z* 287.0921 ([Aglycon − H]$^-$), *m*/*z* 272.0681 ([Aglycon − H]$^-$ − CH_3•), *m*/*z* 245.0126 ($C_9H_9O_6S$), *m*/*z* 229.0108 ($C_9H_9O_5S$), *m*/*z* 177.0598 ($C_{10}H_9O_3$), *m*/*z* 165.0603 ($C_9H_9O_3$), *m*/*z* 163.0388 ($C_9H_7O_3$), *m*/*z* 161.0254 ($C_9H_5O_3$), *m*/*z* 151.0417 ($C_8H_7O_3$,), *m*/*z* 150.0382 ($C_8H_6O_3$), *m*/*z* 149.0653 ($C_9H_9O_2$), 137.0213 ($C_7H_5O_3$), *m*/*z* 135.0589 ($C_8H_7O_2$), *m*/*z* 135.0094 ($C_7H_3O_3$), *m*/*z* 122.0312 ($C_7H_6O_2$) and *m*/*z* 121.0363 ($C_7H_5O_2$) in MS^2 spectra. According to the fragment ion at *m*/*z* 122.0312 ($C_7H_6O_2$), produced from *m*/*z* 272.0681 ([Aglycon − H]$^-$ − CH_3•), we determined that the aglycon of **M114** should be **O** or **P**. Moreover, based on the fragment ion at *m*/*z* 135.0094 ($C_7H_3O_3$), we could deduce that the aglycon of **M114** was **O2** or **P**. However, because the same fragment ions could be produced from **O2** or **P**, it was impossible to judge the position of hydroxylation based on the current mass spectrometry data. In addition, the elemental composition of *m*/*z* 229.0108 ($C_9H_9O_5S$) suggested that the sulfonic group was connected to the fragment ion of *m*/*z* 149.0653 ($C_9H_9O_2$). Hence, we could determine the sulfate was linked to the hydroxyl group of B ring. The MS^2 spectrum of **M114** is shown in Figure S49.

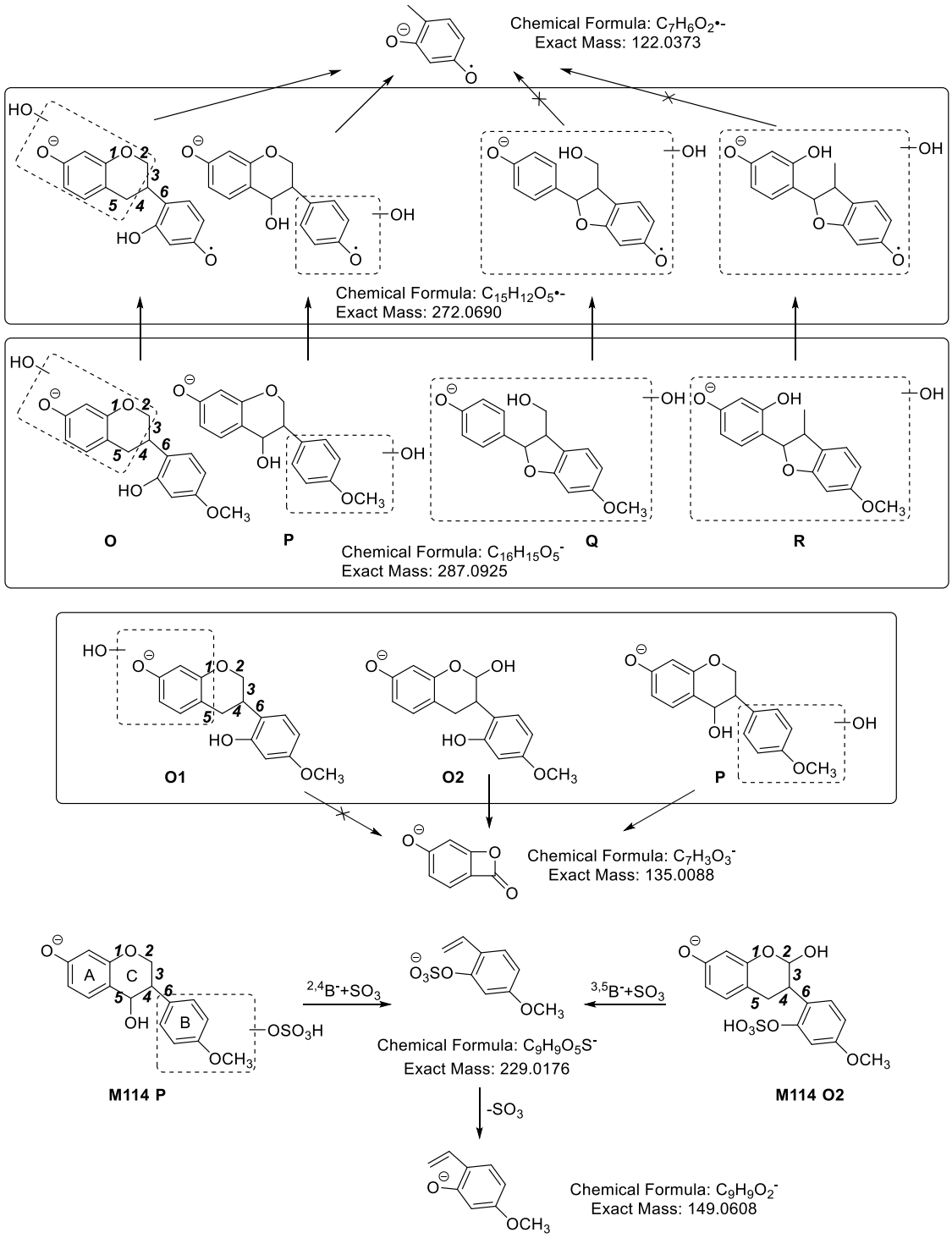

Figure 10. The proposed fragmentation pathways of **M114**.

M115 exhibited fragment ions at *m*/*z* 287.0918 ($C_{16}H_{15}O_5$, [Aglycon – H]$^-$), *m*/*z* 230.9941 ($C_8H_7O_6S$, $^{3,4}B^-$ + SO_3), *m*/*z* 177.0590 ($C_{10}H_9O_3$, $^{2,5}B^-$ – 2H), *m*/*z* 165.0631 ($C_9H_9O_3$, $^{3,5}B^-$ or $^{2,4}B^-$), *m*/*z* 151.0440 ($C_8H_7O_3$, $^{3,4}B^-$), *m*/*z* 150.0407 ($C_9H_9O_3$, $^{3,5}B^-$ – CH_3• or $^{2,4}B^-$ – CH_3•), *m*/*z* 147.0412 ($C_9H_7O_2$, $^6A^-$ – H), *m*/*z* 139.0448 ($C_7H_7O_3$, $^6B^-$ + H), *m*/*z* 136.0182 ($C_7H_4O_3$, $^{3,4}B^-$ – CH_3•), *m*/*z* 135.0397 ($C_8H_7O_2$, $^{3,4}A^-$) and *m*/*z* 121.0325 ($C_7H_5O_2$, $^{3,5}A^-$ or $^{2,4}A^-$) in its MS^2 spectra. From the characteristic fragment ion at *m*/*z* 136.0182 ($C_7H_4O_3$, $^{3,4}B^-$ – CH_3•) yielded from *m*/*z* 151.0440 ($C_8H_7O_3$, $^{3,4}B^-$), we could identify that the newly added hydroxyl group was linked to the D ring of medicarpin and the C11-C11a bond

of medicarpin was cleaved. Moreover, *m/z* 230.9941 was predicted to be $C_8H_7O_6S$, which indicated that the sulfonic group was connected to the fragment ion of *m/z* 151.0440 ($C_8H_7O_3$, $^{3,4}B^-$). We therefore confirmed that the sulfonic group was linked to the hydroxyl group of B ring. The probable structure and characteristic fragment ions of **M115** are shown in Figure 11. The MS^2 spectrum of **M115** is shown in Figure S50.

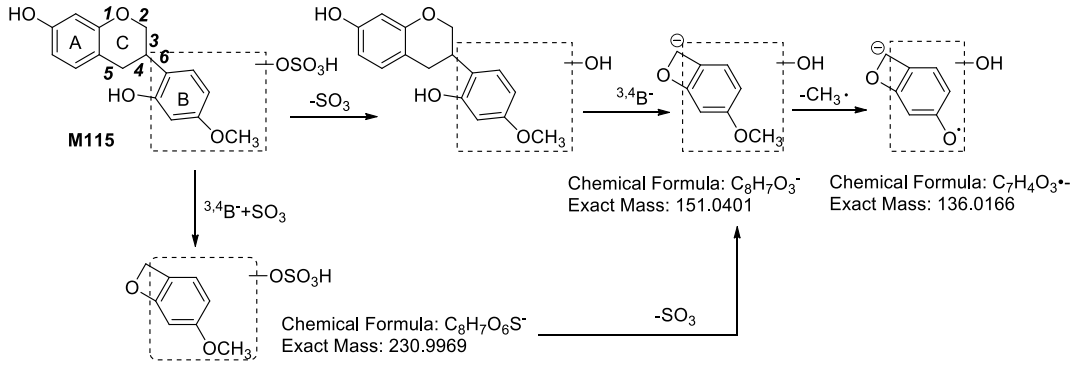

Figure 11. The probable structure and characteristic fragment ions of **M115**.

By comparing the fragmentation pathways of **M112**, **M114** and **M115**, we get the following information: (1) As long as the fragment ion at *m/z* 125.02 ($C_6H_5O_3$) is detected, we can deduce that the newly added hydroxyl group is linked to the A ring; (2) If the fragment ions at *m/z* 151.04 and *m/z* 136.02 are observed at the same time, we can confirm that the newly added hydroxyl group is attached to the D ring of medicarpin and the ring cleavage is at the bond of C11-C11a.

2.2.8. Analysis of Metabolites (**M139**–**M149**) Having the Skeleton of Demethylated, Hydrogenated and Hydroxylated Medicarpin

M140–**M146** showed $[M - H]^-$ at *m/z* 353.03, thus their molecular formulae were identified as $C_{15}H_{14}O_8S$. In their MS^2 spectra, *m/z* 273.08 ($C_{15}H_{13}O_5$) generated by a neutral loss 79.95 Da (SO_3) was detected. Hence, **M140**–**M146** were demethylated, hydrogenated and hydroxylated medicarpin sulfates.

M144 yielded a series of characteristic fragment ions at *m/z* 273.0782 ([Aglycon − H]$^-$), *m/z* 163.0437 ($C_9H_7O_3$), *m/z* 161.0315 ($C_9H_5O_3$), *m/z* 151.0428 ($C_8H_7O_3$), *m/z* 147.0451 ($C_9H_7O_2$), *m/z* 137.0308 ($C_7H_5O_3$), and *m/z* 121.0276 ($C_7H_5O_2$). Based on the fragment ion at *m/z* 151.0428 ($C_8H_7O_3$), we could deduce that the aglycon of **M144** might be **O**, **P**, **Q**, **R**, **S** or **T**. According to the fragment ion at *m/z* 147.0451 ($C_9H_7O_2$), we could exclude **P**, **R** and **T**. Besides, based on the fragment ion at *m/z* 137.0308 ($C_7H_5O_3$), we could exclude **E**. Therefore, we could determine that the aglycon of **M144** was **O** or **Q**. Furthermore, based on the fragment ion at *m/z* 147.0451 ($C_9H_7O_2$), we finally deduced that the aglycon of **M144** was **O1**, **O2** or **Q** (Figure 12). The MS^2 spectrum of **M144** is shown in Figure S51.

The molecular formulae of **M147**–**M149** were predicted as $C_{21}H_{22}O_{11}$ in line with $[M - H]^-$ at *m/z* 449.11. The fragment ion at *m/z* 273.08 ($C_{15}H_{13}O_5$) formed by losing 176.03 Da ($C_6H_8O_6$) from $[M - H]^-$ was detected in the MS^2 spectra. Hence, **M147**–**M149** were demethylated, hydrogenated and hydroxylated medicarpin glucuronides.

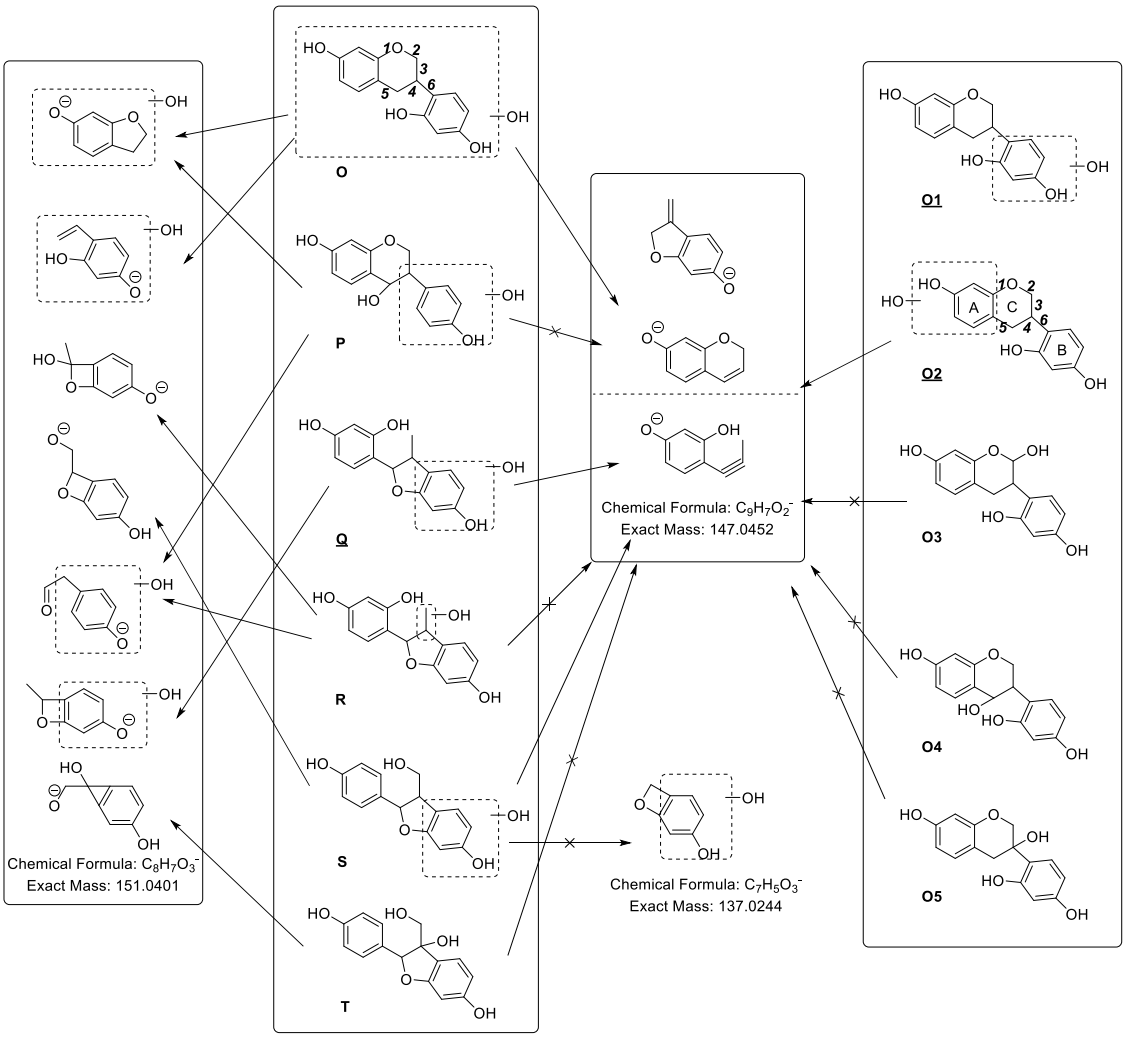

Figure 12. The probable structures (**O1**, **O2**, **Q**) of the aglycon of **M144**.

2.2.9. Analysis of Metabolites (**M150**–**M156**) Having the Skeleton of Demethylated and Dihydroxylated Medicarpin

M150–**M151** showed $[M - H]^-$ at *m*/*z* 463.09 and the molecular formulae were calculated to be $C_{21}H_{20}O_{10}$. **M152**–**M156** showed $[M - H]^-$ at *m*/*z* 367.01, indicating the molecular formulae of $C_{15}H_{12}O_9S$. In their MS^2 spectra, the fragment ion at *m*/*z* 287.06 ($C_{15}H_{11}O_6$) was detected. Compared with $C_{16}H_{14}O_4$ of medicarpin, it had a less CH_2 and two more oxygen atoms. As a result, medicarpin might undergo demethylation and dihydroxylation. Therefore, **M150**–**M151** were glucuronides of demethylated and dehydroxylated medicarpin, while **M152**–**M156** were sulfates of demethylated and dehydroxylated medicarpin.

2.2.10. Analysis of Metabolites (**M157**–**M161**) Having the Skeleton of Dihydroxylated Medicarpin

M157–**M159** showed $[M - H]^-$ at *m*/*z* 381.03 and their molecular formulae were determined as $C_{16}H_{14}O_9S$. In MS^2 spectra, *m*/*z* 381.03 produced $[Aglycon - H]^-$ at *m*/*z* 301.07 ($C_{16}H_{13}O_6$) by the loss of 79.95 Da (SO_3). The elemental composition difference between medicarpin ($C_{16}H_{14}O_4$) and the aglycon of **M157**–**M159** was O_2. Therefore, **M157**–**M159** were identified as sulfates of dihydroxylated medicarpin. In MS^2 spectra of **M159**, fragment ions at *m*/*z* 366.0054 ($C_{15}H_{10}O_9S$, $[M - H]^- - CH_3\bullet$), *m*/*z* 301.0711 ($[Aglycon - H]^-$), *m*/*z* 286.0477 ($[Aglycon - H]^- - CH_3\bullet$) and *m*/*z* 203.9750 ($C_6H_4O_6S$, $^{6,7}D^- + 2H + SO_3$) were detected. Subsequently, *m*/*z* 286.0477 yielded a series of fragment ions at *m*/*z* 162.0347 ($C_9H_6O_3$, $^{2,5}D^- - CH_3\bullet$), *m*/*z* 161.0269 ($C_9H_5O_3$, $^{6,7}A^- - 2H$), *m*/*z* 149.0301 ($C_8H_5O_3$, $^{3,4,7}A^- - H$), *m*/*z*

137.0229 ($C_7H_5O_3$, $^{3,5}A^-$), *m/z* 133.0328 ($C_8H_5O_2$, $^{6,7}A^-$ − 2H − CO), *m/z* 124.0254 ($C_6H_4O_3$, $^{6,7}D^-$ + 2H − CH_3•) and *m/z* 123.0137 ($C_6H_3O_3$, $^{2,5}A^-$). Based on the fragment ion at *m/z* 123.0137 ($C_6H_3O_3$, $^{2,5}A^-$), we assured that one hydroxyl group must be linked to the A ring. Besides, the fragment ion at *m/z* 124.0254 ($C_6H_4O_3$, $^{6,7}D^-$ + 2H − CH_3•) suggested that one hydroxyl group must be linked to the D ring. Furthermore, according to the fragment ion at *m/z* 203.9750 ($C_6H_4O_6S$), we could determine that the sulfonic group was linked to the hydroxyl group of D ring. The fragmentation pathways of **M159** are shown in Figure 13. The MS spectrum of **M159** is shown in Figure S52.

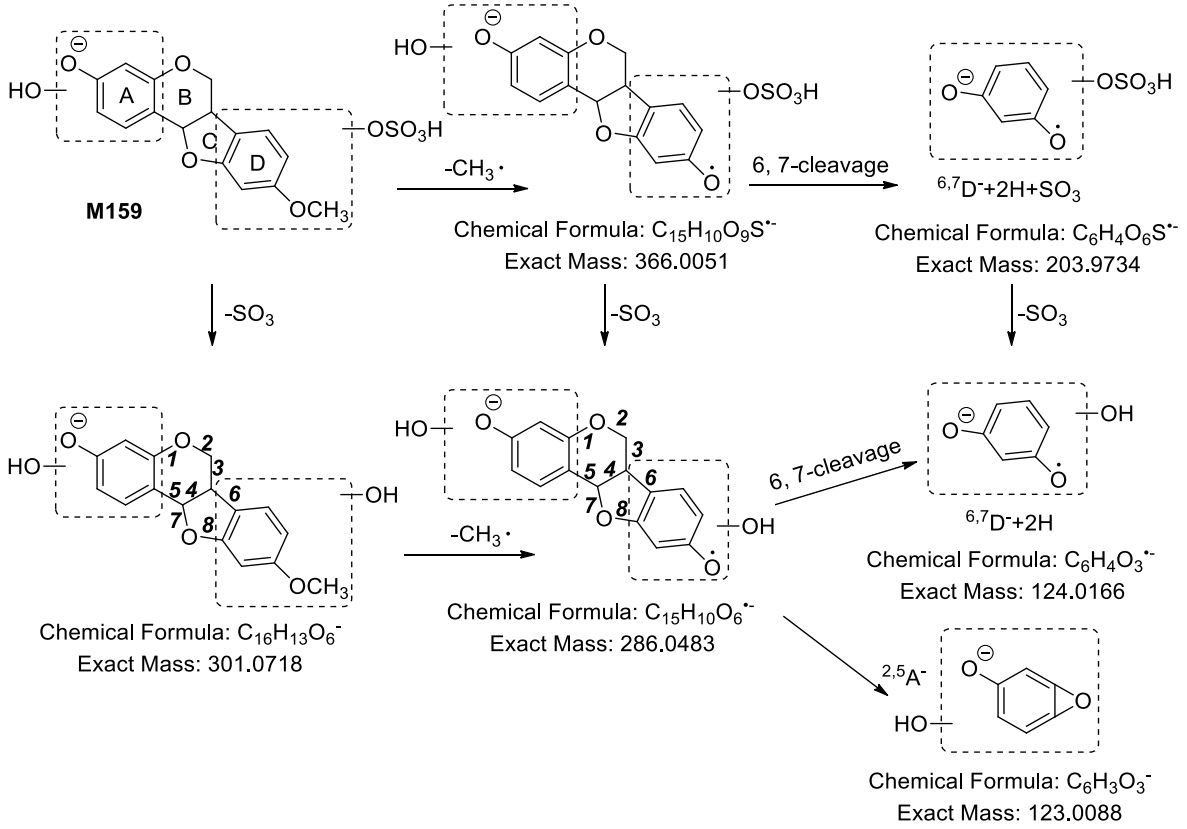

Figure 13. The proposed fragmentation pathways of **M159**.

2.2.11. Analysis of Metabolites M162 Having the Skeleton of Hydrogenated and Dihydroxylated Medicarpin

Its molecular formula was calculated to be $C_{16}H_{16}O_6$ based on $[M - H]^-$ at *m/z* 303.0861. Compared with the $C_{16}H_{14}O_4$ of medicarpin, it had two more hydrogen atoms and two more oxygen atoms. Accordingly, **M162** was determined as hydrogenated and dihydroxylated medicarpin.

2.2.12. Analysis of Metabolites **M163**–**M164** Having the Skeleton of Hydrogenated and Trihydroxylated Medicarpin

M163 showed $[M - H]^-$ at *m/z* 399.0528 and its molecular formula was predicted to be $C_{16}H_{16}O_{10}S$. In its MS^2 spectra, fragment ions at *m/z* 381.0296 ($C_{16}H_{13}O_9S$), *m/z* 301.0664 ($C_{16}H_{13}O_6$) and *m/z* 286.0504 ($C_{15}H_{10}O_6$) were detected. Therefore, **M163** was regarded as hydrogenated and trihydroxylated medicarpin sulfate. The molecular formula of **M164** was calculated to be $C_{17}H_{18}O_{10}S$ based on $[M - H]^-$ at *m/z* 413.0521. In its MS^2 spectra, fragment ions at *m/z* 381.0275 ($C_{16}H_{13}O_9S$), *m/z* 301.0671 ($C_{16}H_{13}O_6$) and *m/z* 286.0517 ($C_{15}H_{10}O_6$) were detected. Therefore, **M164** was determined as hydrogenated, trihydroxylated and methylated medicarpin sulfate.

2.2.13. Analysis of Metabolite **M165** Having the Skeleton of Demethylated, Hydrogenated and Dihydroxylated Medicarpin

M165 showed $[M - H]^-$ at *m*/*z* 369.0297 and its molecular formula was predicted to be $C_{15}H_{14}O_9S$. In its MS^2 spectra, fragment ions at *m*/*z* 351.0135 ($C_{15}H_{11}O_8S$) and *m*/*z* 271.0607 ($C_{15}H_{11}O_5$) were detected, indicating two sequential neutral losses of 18.01 Da (H_2O) and 79.95 Da (SO_3). Compared with $C_{16}H_{13}O_4$ of medicarpin, *m*/*z* 271.0607 had a less CH_2 and one more oxygen atom. Therefore, **M165** was determined as a demethylated, hydrogenated and dihydroxylated medicarpin sulfate.

2.3. Distribution of 165 Metabolites in Rats

The distribution of 165 metabolites (including 104 metabolites in urine, 29 metabolites in feces, 38 metabolites in plasma, 41 metabolites in the colon, 74 metabolites in the intestine, 28 metabolites in the stomach, 24 metabolites in the liver, 15 metabolites in the spleen, 42 metabolites in the kidney, 8 metabolites in the lung, 10 metabolites in the heart, 3 metabolites in the brain and 17 metabolites in the thymus) of medicarpin and their relative contents in each biological sample are shown in Figure 14. The relative content of a metabolite in each biosample was calculated by (peak area of a metabolite in the sample/total peak area of all metabolites detected in the sample) × 100%. The peak area of a metabolite was calculated from its extracted ion chromatogram.

From Figure 14, we could find that: (1) in urine, **M159** (12.68%, dihydroxylated medicarpin sulfate), **M63** (11.86%, demethylated and hydroxylated medicarpin sulfate), **M17** (7.18%, demethylated medicarpin sulfate), and **M64** (5.34%) were four major metabolites and all of them were sulfates; it is an interesting phenomenon that sulfates other than glucuronides are major metabolites in urine, and the cause is unclear; (2) in feces, **M18** (20.34%), **M43** (10.35%), **M34** (9.89%), **M40** (8.86%), **M3** (7.57%, Vc conjugate), and **M27** (7.25%) were six major metabolites with a relative content higher than 5%, and three of them (**M43**, **M34**, **M40**) were demethylated and hydrogenated medicarpin sulfates; (3) in plasma, **M1** (36.15%, medicarpin glucuronide), **M5** (12.82%, vestitol-1′-*O*-glucuronide), **M18** (10.81%), **M65** (8.00%),and **M40** (5.58%) were major metabolites; (4) **M1** was the most abundant metabolite in the stomach, liver, spleen, kidney, lung, heart, and thymus. **M5**, **M14** (demethylated medicarpin) were the most abundant metabolites in intestine and liver, respectively. **M17** (demethylated medicarpin sulfate) was the most abundant metabolite in the colon and brain; (5) **M1**, **M5** were detected in all 10 organs; **M30** (demethylated and hydrogenated medicarpin glucuronide) was detected in nine organs (except the brain); **M12** and **M27** were detected in eight organs; therefore, these five metabolites were widely distributed in vivo. Considering the high abundance and wide distribution, we suggest that the bioactivities of these metabolites deserve further research in order to fully explain the pharmacological action mechanism of medicarpin. In addition, the reason for specific distribution of some metabolites (e.g., **M2**, **M14**, **M20**, **M35**, **M40**, **M54**, **M109**) also need further investigation.

The metabolic reactions of medicarpin included demethylation, hydrogenation, hydroxylation, glucuronidation, sulfation, glycosylation, methylation, and conjunction of vitamin C. The relative contents of metabolic reactions and phase I metabolites in each biosample are shown in Table 1, which were calculated by summing the relative contents of all metabolites generated through it and all phase I metabolites, respectively. In urine, the contents of sulfation metabolites, glucuronidation metabolites and vitamin C conjugates were 74.60%, 25.83% and 1.08%, respectively. In feces, the contents of sulfation metabolites, glucuronidation metabolites and vitamin C conjugates were 73.53%, 1.62% and 15.54%, respectively. This indicated that medicarpin was mainly excreted in the form of sulfates. In plasma, the major metabolic reaction was glucuronidation (relative content: 67.87%). The glycosylation metabolite (**M50**) was only found in urine. Furthermore, the contents of phase I metabolites of medicarpin in most biosamples were very low (<10%), except in the colon (17.57%), which suggested that phase II metabolites are major metabolites.

No.	$t_{R(min)}$	Identification	Meas. mass	Pred. mass	Molecular Formula	Error (ppm)	DBE	MS fragments	urine	feces	plasma	colon	intestine	stomach	liver	spleen	kidney	lung	heart	brain	thymus
M1	96.358	+GlcUA	445.1174	445.1140	$C_{22}H_{22}O_{10}$	7.64	12	269.0788;175.0260	1.85%	-	36.15%	8.41%	1.35%	39.10%	21.10%	56.63%	18.05%	56.70%	59.46%	22.03%	63.63%
M2	98.795	+GlcUA	445.1135	445.1140	$C_{22}H_{22}O_{10}$	-1.12	12	269.0838	-	-	-	-	6.14%	-	-	-	-	-	-	-	-
M3[a]	104.382	+Vc	427.1049	427.1035	$C_{22}H_{20}O_9$	3.28	13	269.0792;254.0562	0.91%	7.57%	0.44%	1.87%	2.51%	0.64%	-	-	0.10%	-	-	-	-
M4	112.168	+2H	271.0979	271.0976	$C_{16}H_{16}O_4$	1.11	9	147.0469;135.0466;123.0543; 121.0302;109.0321	0.87%	-	-	4.66%	0.31%	0.64%	-	-	-	-	-	-	-
M5[a]	90.033	+2H,+GlcUA	447.1314	447.1297	$C_{22}H_{24}O_{10}$	3.80	11	271.0962;175.0245;147.0527; 135.0519	3.54%	-	12.82%	3.09%	10.33%	4.99%	7.54%	7.37%	7.55%	9.05%	6.80%	20.86%	5.79%
M6[a]	92.050	+2H,+GlcUA	447.1323	447.1297	$C_{22}H_{24}O_{10}$	5.81	11	271.0944;175.0255;147.0527; 135.0498	1.66%	-	0.68%	0.26%	2.94%	0.67%	1.01%	0.52%	0.85%	-	-	-	0.63%
M7[a]	77.292	+2H,+2GlcUA	623.1631	623.1618	$C_{28}H_{32}O_{16}$	2.09	13	447.1258;271.0873	0.16%	-	-	-	-	-	-	-	-	-	-	-	-
M8[a]	97.308	+2H,+Vc	429.1232	429.1191	$C_{22}H_{22}O_9$	9.55	12	271.0945;147.0469;135.0644	-	0.89%	-	1.14%	0.15%	-	-	-	-	-	-	-	-
M9[a]	98.833	+2H,+Vc	429.1232	429.1191	$C_{22}H_{22}O_9$	9.55	12	271.0967;147.0515;135.0524	0.17%	2.99%	-	3.76%	2.52%	0.59%	-	-	-	-	-	-	-
M10[a]	114.015	+2H,+SO_3,+GlcUA	527.0885	527.0865	$C_{22}H_{24}O_{13}S$	3.79	11	351.0539;271.0956;147.0496; 135.0471;121.0302	1.34%	-	2.69%	-	1.84%	-	-	-	0.14%	-	-	-	-
M11	58.417	-CH_3,+GlcUA	431.0988	431.0984	$C_{21}H_{20}O_{10}$	0.93	12	255.0664	0.02%	-	-	-	0.03%	-	-	-	-	-	-	-	-
M12	67.275	-CH_3,+GlcUA	431.1009	431.0984	$C_{21}H_{20}O_{10}$	5.80	12	255.0653;175.0264	1.15%	-	4.79%	0.36%	3.83%	1.21%	1.17%	-	1.55%	2.67%	2.24%	-	2.11%
M13	68.442	-CH_3,+GlcUA	431.1019	431.0984	$C_{21}H_{20}O_{10}$	8.12	12	255.0665;175.0345	1.22%	-	1.12%	0.50%	4.25%	1.45%	1.22%	0.61%	1.25%	-	-	-	1.62%
M14[a]	111.653	-CH_3,+SO_3	335.0241	335.0231	$C_{15}H_{12}O_7S$	2.98	10	255.0658;145.0354;133.0388; 121.0341	-	-	-	-	-	-	31.83%	-	-	-	-	-	-
M15[a]	113.593	-CH_3,+SO_3	335.0245	335.0231	$C_{15}H_{12}O_7S$	4.18	10	255.0686	-	-	-	-	-	-	0.76%	-	-	-	-	-	-
M16[a]	115.450	-CH_3,+SO_3	335.0232	335.0231	$C_{15}H_{12}O_7S$	0.30	10	255.0667;121.0293	-	-	-	-	-	-	-	-	-	12.43%	-	-	-
M17[a]	119.148	-CH_3,+SO_3	335.0234	335.0231	$C_{15}H_{12}O_7S$	0.90	10	255.0661;145.0317;133.0350; 121.0336	7.18%	-	-	14.57%	1.09%	-	-	10.57%	-	-	9.37%	57.11%	-
M18[a]	121.107	-CH_3,+SO_3	335.0221	335.0231	$C_{15}H_{12}O_7S$	-2.98	10	255.0639;145.0267;133.0298; 121.0365	4.07%	20.34%	10.81%	-	3.76%	17.14%	-	-	17.09%	-	-	-	7.86%
M19[a]	124.552	-CH_3,+SO_3	335.0253	335.0231	$C_{15}H_{12}O_7S$	6.57	10	255.0669;121.0302	-	1.37%	0.35%	-	-	-	-	-	-	-	-	-	-
M20[a]	132.978	-CH_3,+SO_3	335.0235	335.0231	$C_{15}H_{12}O_7S$	-6.27	10	255.0637	0.80%	-	-	-	-	-	-	-	0.59%	-	-	-	-
M21[a]	81.330	-CH_3,+SO_3,+GlcUA	511.0584	511.0552	$C_{21}H_{20}O_{13}S$	6.26	12	335.0243;255.0734	-	-	-	-	8.30%	-	-	-	-	-	-	-	-
M22[a]	82.158	-CH_3,+SO_3,+GlcUA	511.0586	511.0552	$C_{21}H_{20}O_{13}S$	6.65	12	335.0177;255.0651;145.0269; 121.0197	0.22%	-	-	-	-	-	-	-	-	-	-	-	-
M23[a]	84.255	-CH_3,+SO_3,+GlcUA	511.0530	511.0552	$C_{21}H_{20}O_{13}S$	-4.30	12	335.0180;255.0516	-	-	-	-	0.17%	-	-	-	-	-	-	-	-
M24	76.325	-CH_3,+Vc	413.0950	413.0878	$C_{21}H_{18}O_9$	4.12	13	255.0639	-	0.96%	-	0.39%	0.12%	-	-	-	-	-	-	-	-
M25	76.910	-CH_3,+Vc	413.0892	413.0878	$C_{21}H_{18}O_9$	3.39	13	255.0653	-	-	-	-	0.07%	-	-	-	-	-	-	-	-
M26[a]	96.495	-CH_3,+SO_3,+Vc	493.0438	493.0446	$C_{21}H_{18}O_{12}S$	-1.62	13	413.0876;255.0641	-	-	-	-	0.54%	-	-	-	-	-	-	-	-
M27	83.117	-CH_3,+2H	257.0820	257.0819	$C_{15}H_{14}O_4$	0.39	9	149.0289;147.0481;135.0494; 121.0329;109.0263	0.36%	7.25%	-	8.32%	0.44%	0.85%	0.80%	0.88%	0.17%	-	0.54%	-	0.49%
M28	53.108	-CH_3,+2H,+GlcUA	433.1165	433.1140	$C_{21}H_{22}O_{10}$	5.77	11	175.024	0.10%	-	-	-	0.06%	-	-	-	-	-	-	-	-
M29	64.033	-CH_3,+2H,+GlcUA	433.1156	433.1140	$C_{21}H_{22}O_{10}$	3.69	11	257.0822;175.0246	0.40%	-	-	0.26%	2.30%	0.52%	0.98%	0.67%	1.01%	-	-	-	-
M30	70.067	-CH_3,+2H,+GlcUA	433.1152	433.1140	$C_{21}H_{22}O_{10}$	2.77	11	257.0812;175.0253;147.0565	1.01%	-	-	1.02%	3.95%	1.55%	3.05%	3.64%	1.93%	3.35%	3.20%	-	2.07%
M31	73.850	-CH_3,+2H,+GlcUA	433.1142	433.1140	$C_{21}H_{22}O_{10}$	0.46	11	257.0793;175.0265;147.0552; 135.0461	1.40%	-	0.44%	0.13%	2.01%	0.33%	-	0.26%	0.76%	-	-	-	-

Figure 14. *Cont.*

No.	$t_{R(min)}$	Identification	Meas. mass	Pred. mass	Molecular Formula	Error (ppm)	DBE	MS fragments	urine	feces	plasma	colon	intestine	stomach	liver	spleen	kidney	lung	heart	brain	thymus
M32[a]	62.508	-CH_3,+2H,+SO_3	337.0386	337.0387	$C_{15}H_{14}O_7S$	-0.30	9	257.0826;147.0478;135.0500; 133.0305;121.0306	-	4.40%	-	-	-	-	-	-	-	-	-	-	-
M33[a]	100.325	-CH_3,+2H,+SO_3	337.0397	337.0387	$C_{15}H_{14}O_7S$	2.97	9	257.0787;147.0605;135.0489; 121.0262	-	-	-	-	-	-	6.23%	-	-	-	-	-	-
M34[a]	106.490	-CH_3,+2H,+SO_3	337.0378	337.0387	$C_{15}H_{14}O_7S$	-2.67	9	257.0807;147.0483;135.0489; 121.0328	4.44%	9.89%	-	7.65%	2.56%	1.80%	-	1.64%	2.70%	-	3.23%	-	1.51%
M35[a]	110.073	-CH_3,+2H,+SO_3	337.0391	337.0387	$C_{15}H_{14}O_7S$	0.89	9	257.0806;147.0561;135.0437; 121.0355	-	-	-	-	-	-	4.00%	-	-	-	-	-	-
M36[a]	114.563	-CH_3,+2H,+SO_3	337.0404	337.0387	$C_{15}H_{14}O_7S$	5.04	9	257.0816;147.0491;135.0509; 121.0431	-	-	-	-	-	-	6.99%	-	-	6.14%	-	-	-
M37[a]	116.257	-CH_3,+2H,+SO_3	337.0392	337.0387	$C_{15}H_{14}O_7S$	1.48	9	257.0804;147.0456;135.0461; 121.0267;119.0586;109.0234	2.51%	-	-	5.24%	-	-	-	-	-	-	4.55%	-	-
M38[a]	117.398	-CH_3,+2H,+SO_3	337.0404	337.0387	$C_{15}H_{14}O_7S$	4.15	9	257.0814;147.0463;135.0473; 121.0354;109.0277	0.71%	-	-	-	-	-	-	-	5.62%	-	-	-	-
M39[a]	118.565	-CH_3,+2H,+SO_3	337.0415	337.0387	$C_{15}H_{14}O_7S$	8.31	9	257.0804;135.0451;121.0293	-	-	-	-	-	-	-	-		4.37%	-	-	2.84%
M40[a]	119.658	-CH_3,+2H,+SO_3	337.0386	337.0387	$C_{15}H_{14}O_7S$	-0.30	9	257.0808;151.0405;147.0447; 135.0441;121.0348	-	8.86%	5.58%	-	-	-	-	4.42%		-	-	-	-
M41[a]	121.218	-CH_3,+2H,+SO_3	337.0354	337.0387	$C_{15}H_{14}O_7S$	-9.79	9	257.0753;151.0463;147.0507; 135.0456	-	-	-	8.28%	-	-	-	-		-	4.42%	-	-
M42[a]	87.040	-CH_3,+2H,+SO_3	337.0392	337.0387	$C_{15}H_{14}O_7S$	1.48	9	257.0804	-	-	-	-	-	-	-	-	0.57%	-	-	-	-
M43[a]	123.557	-CH_3,+2H,+SO_3	337.0378	337.0387	$C_{15}H_{14}O_7S$	4.75	9	257.0806;147.0491;135.0491; 121.0341	3.74%	10.35%	-	-	-	1.84%	-	4.06%	5.16%	-	-	-	2.33%
M44[a]	85.117	-CH_3,+2H,+2SO_3	416.9988	416.9956	$C_{15}H_{14}O_{10}S_2$	0.00	9	337.0389;257.0978	1.12%	-	-	-	-	-	-	-	-	-	-	-	-
M45	58.475	-CH_3,+2H,+2GlcUA	609.1475	609.1461	$C_{27}H_{30}O_{16}$	2.30	13	433.1137;257.0857	0.20%	-	-	-	-	-	-	-	-	-	-	-	-
M46[a]	82.667	-CH_3,+2H,+SO_3,+GlcUA	513.0733	513.0708	$C_{21}H_{22}O_{13}S$	4.87	11	433.1191;337.0383;257.0831; 151.0359;135.0465;133.0249; 121.0302	0.37%	-	0.92%	-	0.29%	-	-	-	-	-	-	-	-
M47[a]	90.667	-CH_3,+2H,+SO_3,+GlcUA	513.0718	513.0708	$C_{21}H_{22}O_{13}S$	1.95	11	433.1126;337.0369;257.0791; 135.0487;121.0361	0.23%	-	0.09%	-	0.27%	-	-	-	-	-	-	-	-
M48[a]	92.842	-CH_3,+2H,+SO_3,+GlcUA	513.0717	513.0708	$C_{21}H_{22}O_{13}S$	1.75	11	337.0378;257.0854;147.0527; 135.0523;121.0406	0.22%	-	-	-	0.51%	-	-	-	-	-	-	-	-
M49[a]	83.662	-CH_3,+2H,+SO_3,+GlcUA	513.0693	513.0708	$C_{21}H_{22}O_{13}S$	-2.92	11	337.0372;257.0750	-	-	0.35%	-	-	-	-	-	-	-	-	-	-
M50[a]	85.750	-CH3,+2H,+SO_3,+Glc	499.0941	499.0916	$C_{21}H_{24}O_{12}S$	5.01	10	337.0367;257.0800;147.0373	0.23%	-	-	-	-	-	-	-	-	-	-	-	-
M51	74.183	-CH_3,+2H,+Vc	415.1075	415.1035	$C_{21}H_{20}O_9$	9.64	12	257.0817;147.0498	-	0.47%	-	0.41%	0.22%	-	-	-	-	-	-	-	-
M52	78.900	-CH_3,+2H,+Vc	415.1057	415.1035	$C_{21}H_{20}O_9$	5.30	12	257.0794;147.0498;135.0534	-	1.50%	-	1.39%	0.70%	-	-	-	-	-	-	-	-
M53	71.658	-CH_3,+OH	271.0613	271.0612	$C_{15}H_{12}O_5$	0.37	10	161.0281;137.0283;133.0249; 121.0406;109.0327	0.07%	1.01%	-	-	-	-	-	-	-	-	-	-	-
M54[a]	41.187	-CH_3,+OH,+SO_3	351.0160	351.0180	$C_{15}H_{12}O_8S$	-5.70	10	271.0538	-	-	-	0.43%	-	-	-	-	-	-	-	-	-
M55[a]	60.743	-CH_3,+OH,+SO_3	351.0195	351.0180	$C_{15}H_{12}O_8S$	4.27	10	271.0731	-	-	-	-	-	-	0.42%	-	-	-	-	-	-
M56[a]	66.033	-CH_3,+OH,+SO_3	351.0200	351.0180	$C_{15}H_{12}O_8S$	5.70	10	271.0624;253.0485;161.0375; 135.0424;133.0358	0.11%	-	-	-	0.13%	-	-	-	-	-	-	-	-
M57[a]	74.340	-CH_3,+OH,+SO_3	351.0213	351.0180	$C_{15}H_{12}O_8S$	9.40	10	271.0719;161.0247	-	-	-	-	-	-	1.80%	-	-	-	-	-	-
M58[a]	79.593	-CH_3,+OH,+SO_3	351.0166	351.0180	$C_{15}H_{12}O_8S$	-3.99	10	271.0549;161.0239		-	-	0.38%	0.22%	-	-	-	1.29%	-	-	-	-

Figure 14. *Cont.*

No.	$t_{R(min)}$	Identification	Meas. mass	Pred. mass	Molecular Formula	Error (ppm)	DBE	MS fragments	urine	feces	plasma	colon	intestine	stomach	liver	spleen	kidney	lung	heart	brain	thymus
M59[a]	80.375	-CH_3,+OH,+SO_3	351.0181	351.0180	$C_{15}H_{12}O_8S$	0.28	10	271.0633;253.0495;243.0637; 161.0267;133.0305;121.0242	2.06%	-	0.78%	-	0.07%	-	-	-	-	-	-	-	-
M60[a]	107.480	-CH_3,+OH,+SO_3	351.1062	351.0180	$C_{15}H_{12}O_8S$	-5.13	10	271.0629;161.0244	-	-	0.67%	-	-	-	-	-	-	-	-	-	-
M61[a]	109.963	-CH_3,+OH,+SO_3	351.0176	351.0180	$C_{15}H_{12}O_8S$	-1.14	10	271.0640;161.0362	-	-	-	-	-	-	1.40%	-	-	-	-	-	-
M62[a]	114.665	-CH_3,+OH,+SO_3	351.0179	351.0180	$C_{15}H_{12}O_8S$	-0.28	10	271.0590;253.0466;161.0234; 149.0232;121.0406	0.66%	-	-	-	-	-	-	-	0.48%	5.29%	-	-	-
M63[a]	117.457	-CH_3,+OH,+SO_3	351.0178	351.0180	$C_{15}H_{12}O_8S$	-0.57	10	271.0602;253.0495;161.0276; 149.0255;133.0334;121.0406	11.86%	-	-	2.67%	0.34%	-	1.97%	-	12.87%	-	6.19%	-	3.15%
M64[a]	120.298	-CH_3,+OH,+SO_3	351.0180	351.0180	$C_{15}H_{12}O_8S$	0.00	10	271.0598;253.0502;161.0281; 147.0425;133.0321;121.0302	5.34%	-	-	-	1.75%	12.76%	-	7.11%	7.07%	-	-	-	1.27%
M65[a]	122.517	-CH_3,+OH,+SO_3	351.0212	351.0180	$C_{15}H_{12}O_8S$	9.12	10	271.0606;253.0561;161.0182	-	1.44%	8.00%	-	-	-	-	-	-	-	-	-	-
M66[a]	126.180	-CH_3,+OH,+SO_3	351.0180	351.0180	$C_{15}H_{12}O_8S$	0.00	10	271.0615;253.0511;161.0271; 121.0322	0.72%	-	-	0.55%	-	-	-	-	0.57%	-	-	-	-
M67[a]	128.858	-CH_3,+OH,+SO_3	351.0162	351.0180	$C_{15}H_{12}O_8S$	-5.13	10	271.0606;253.0582;161.0254	-	2.77%	0.37%	-	-	-	-	-	-	-	-	-	-
M68	64.775	-CH_3,+OH,+GlcUA	447.0943	447.0933	$C_{21}H_{20}O_{11}$	2.24	12	271.0561	0.05%	-	-	-	0.48%	-	-	-	-	-	-	-	-
M69	70.517	-CH_3,+OH,+GlcUA	447.0930	447.0933	$C_{21}H_{20}O_{11}$	-0.67	12	271.0597	0.03%	-	-	-	-	-	-	-	-	-	-	-	-
M70	61.903	-CH_3,+OH,+GlcUA	447.0963	447.0933	$C_{21}H_{20}O_{11}$	6.71	12	271.0561;161.0206	-	-	0.38%	-	-	-	-	-	-	-	-	-	-
M71	68.282	-CH_3,+OH,+GlcUA	447.0928	447.0933	$C_{21}H_{20}O_{11}$	-1.12	12	271.0561;175.0220	-	-	0.68%	-	-	-	-	-	-	-	-	-	-
M72[a]	80.083	-CH_3,+OH,+SO_3,+GlcUA	527.0517	527.0501	$C_{21}H_{20}O_{14}S$	3.04	12	351.0146;271.0604;161.0209	0.38%	-	-	-	0.08%	-	-	-	-	-	-	-	-
M73[a]	87.692	-CH_3,+OH,+SO_3,+GlcUA	527.0530	527.0501	$C_{21}H_{20}O_{14}S$	5.50	12	351.0168;271.0619	0.10%	-	-	-	0.21%	-	-	-	-	-	-	-	-
M74[a]	89.525	-CH_3,+OH,+SO_3,+GlcUA	527.0523	527.0501	$C_{21}H_{20}O_{14}S$	4.17	12	351.0158;271.0618;253.0516; 149.0232	0.05%	-	-	-	-	-	-	-	-	-	-	-	-
M75	57.508	-CH_3,+OH,+2GlcUA	623.1259	623.1254	$C_{27}H_{28}O_{17}$	0.80	14	447.0930;271.0587	0.05%	-	-	-	-	-	-	-	-	-	-	-	-
M76	100.975	+OH	285.0784	285.0768	$C_{16}H_{14}O_5$	5.61	10	270.0518;161.0342	0.07%	1.04%	-	-	-	-	-	-	-	-	-	-	-
M77	114.565	+OH	285.0790	285.0768	$C_{16}H_{14}O_5$	7.72	10	270.0591	0.09%	-	-	-	-	-	-	-	-	-	-	-	-
M78	70.575	+OH,+GlcUA	461.1109	461.1089	$C_{22}H_{22}O_{11}$	4.34	12	285.0753;270.0546;175.0283	0.60%	-	0.38%	-	2.13%	0.28%	0.29%	-	0.25%	-	-	-	0.29%
M79	73.267	+OH,+GlcUA	461.1102	461.1089	$C_{22}H_{22}O_{11}$	2.82	12	285.0752;270.0520;175.0275	0.25%	0.74%	0.14%	0.53%	4.72%	0.93%	0.99%	-	0.42%	-	-	-	1.74%
M80	76.333	+OH,+GlcUA	461.1107	461.1089	$C_{22}H_{22}O_{11}$	3.90	12	285.0764;270.0515;175.0311	0.91%	-	1.30%	0.55%	4.04%	0.52%	1.20%	0.60%	0.67%	-	-	-	0.67%
M81	88.658	+OH,+GlcUA	461.1113	461.1089	$C_{22}H_{22}O_{11}$	5.20	12	285.0761;270.0591;175.0284	1.74%	-	0.07%	1.51%	0.61%	-	-	-	-	-	-	-	-
M82	91.152	+OH,+GlcUA	461.1061	461.1089	$C_{22}H_{22}O_{11}$	-6.07	12	285.0708;270.0515;175.0264	-	-	-	-	0.96%	-	-	-	-	-	-	-	-
M83	94.092	+OH,+GlcUA	461.1101	461.1089	$C_{22}H_{22}O_{11}$	2.60	12	285.0752;270.0526;175.0232	0.25%	-	0.22%	-	0.88%	0.51%	-	-	-	-	-	-	-
M84	94.975	+OH,+GlcUA	461.1091	461.1089	$C_{22}H_{22}O_{11}$	0.43	12	285.0730;270.0513	0.06%	-	0.28%	-	0.42%	-	-	-	-	-	-	-	-
M85	89.400	+OH,+GlcUA	461.1104	461.1089	$C_{22}H_{22}O_{11}$	3.25	12	285.0794	-	0.88%	0.32%	-	-	-	-	-	-	-	-	-	-
M86	79.183	+OH,+2GlcUA	637.1410	637.1410	$C_{28}H_{30}O_{17}$	0.00	14	461.1098;285.0783	0.14%	-	-	-	-	-	-	-	-	-	-	-	-
M87[a]	109.455	+OH,+SO_3	365.0350	365.0337	$C_{16}H_{14}O_8S$	3.56	10	285.0735;270.0503	-	-	-	-	-	-	1.71%	-	-	-	-	-	-
M88[a]	115.090	+OH,+SO_3	365.0331	365.0337	$C_{16}H_{14}O_8S$	-1.64	10	285.0727;270.0564;161.0254; 139.0337;124.0179	0.12%	-	-	-	-	-	-	-	0.19%	-	-	-	-
M89[a]	117.085	+OH,+SO_3	365.0327	365.0337	$C_{16}H_{14}O_8S$	-2.74	10	285.0750;270.0547;	-	3.96%	-	-	-	-	-	-	0.35%	-	-	-	-
M90[a]	119.537	+OH,+SO_3	365.0372	365.0337	$C_{16}H_{14}O_8S$	9.59	10	285.0748;270.0412	-	-	-	0.50%	-	-	-	-	0.92%	-	-	-	-
M91[a]	122.465	+OH,+SO_3	365.0328	365.0337	$C_{16}H_{14}O_8S$	-2.47	10	285.0772;270.0514;161.0194	1.09%	-	2.30%	-	-	-	-	-	-	-	-	-	-
M92[a]	123.285	+OH,+SO_3	365.0352	365.0337	$C_{16}H_{14}O_8S$	4.11	10	285.0707	-	-	-	-	-	-	-	-	0.20%	-	-	-	-
M93[a]	124.448	+OH,+SO_3	365.0335	365.0387	$C_{16}H_{14}O_8S$	-0.55	10	285.0755;270.0502	-	-	-	1.83%	-	-	-	-	-	-	-	-	-

Figure 14. *Cont.*

No.	$t_{R(min)}$	Identification	Meas. mass	Pred. mass	Molecular Formula	Error (ppm)	DBE	MS fragments	urine	feces	plasma	colon	intestine	stomach	liver	spleen	kidney	lung	heart	brain	thymus
M94[a]	126.022	+OH,+SO_3	365.0339	365.0337	$C_{16}H_{14}O_8S$	0.27	10	285.0711;270.0554;161.0295	0.43%	-	-	-	-	-	-	-	-	-	-	-	-
M95[a]	127.867	+OH,+SO_3	365.0328	365.0337	$C_{16}H_{14}O_8S$	-2.47	10	285.0758;270.0512;161.0254	0.25%	1.05%	-	-	-	-	-	-	-	-	-	-	-
M96[a]	137.550	+OH,+SO_3	365.0333	365.0337	$C_{16}H_{14}O_8S$	-1.10	10	285.0737	0.17%	-	-	-	-	-	-	-	-	-	-	-	-
M97[a]	143.963	+OH,+SO_3	365.0326	365.0337	$C_{16}H_{14}O_8S$	-3.01	10	285.0736;270.0529;161.0194; 149.0463	0.20%	-	-	-	-	-	-	-	-	-	-	-	-
M98[a]	66.308	+OH,+SO_3	365.0336	365.0337	$C_{16}H_{14}O_8S$	-0.27	10	285.0750;270.0501	-	0.75%	-	-	-	-	-	-	-	-	-	-	-
M99[a]	82.375	+OH,+SO_3	365.0334	365.0337	$C_{16}H_{14}O_8S$	-0.82	10	285.0815;270.0572	-	3.64%	-	5.45%	-	-	-	-	-	-	-	-	-
M100[a]	95.765	+OH,+SO_3,+GlcUA	541.0654	541.0657	$C_{22}H_{22}O_{14}S$	-0.55	12	365.0300;285.0705	-	-	-	-	0.34%	-	-	-	-	-	-	-	-
M101[a]	96.650	+OH,+SO_3,+GlcUA	541.0679	541.0657	$C_{22}H_{22}O_{14}S$	4.07	12	461.1056;365.0282;285.0711; 270.0510;161.0254;123.0074	0.09%	-	-	-	-	-	-	-	-	-	-	-	-
M102[a]	83.475	+OH,+SO_3,+GlcUA	541.0618	541.0657	$C_{22}H_{22}O_{14}S$	-7.21	12	365.0293;285.0794;270.0497	-	-	0.09%	-	-	-	-	-	-	-	-	-	-
M103[a]	84.813	+OH,+SO_3,+GlcUA	541.0617	541.0657	$C_{22}H_{22}O_{14}S$	-7.39	12	365.0344;285.0724;270.0502	-	-	0.35%	-	0.05%	-	-	-	-	-	-	-	-
M104	78.167	+OH,+Vc	443.0968	443.0984	$C_{22}H_{20}O_{10}$	2.03	13	285.0837;270.0513	-	0.33%	-	0.27%	0.76%	-	-	-	-	-	-	-	-
M105	99.750	+OH,+Vc	443.0976	443.0984	$C_{22}H_{20}O_{10}$	-1.81	13	285.0688	-	0.46%	-	-	-	-	-	-	-	-	-	-	-
M106	95.783	+OH,+CH_2,+GlcUA	475.1247	475.1246	$C_{23}H_{24}O_{11}$	0.21	12	299.0943;175.0288	0.50%	-	0.30%	-	0.92%	0.34%	0.40%	-	0.27%	-	-	-	-
M107	97.575	+OH,+CH_2,+GlcUA	475.1254	475.1246	$C_{23}H_{24}O_{11}$	1.68	12	299.0945;284.0686;175.0233	2.23%	-	2.74%	0.78%	7.26%	1.89%	2.32%	1.03%	0.70%	-	-	-	2.01%
M108	77.457	+2H,+OH	287.0899	287.0925	$C_{16}H_{16}O_5$	-9.06	9	269.0789;254.0372;137.0342	-	-	-	-	0.06%	4.77%	-	-	-	-	-	-	-
M109	79.677	+2H,+OH	287.0908	287.0925	$C_{16}H_{16}O_5$	-5.92	9	269.0832;254.0573;137.0242;	-	-	-	-	-	1.33%	-	-	-	-	-	-	-
M110	83.817	+2H,+OH	287.0932	287.0925	$C_{16}H_{16}O_5$	2.44	9	272.0682;165.0585;163.0545; 150.0231;147.0527;137.0234; 135.0522	0.10%	-	-	1.56%	0.19%	-	-	-	-	-	-	-	-
M111	91.192	+2H,+OH	287.0915	287.0925	$C_{16}H_{16}O_5$	-3.48	9	163.0388;151.0451;149.0532; 145.0348;137.0334;134.0482; 125.0181	0.17%	-	-	-	-	-	-	-	-	-	-	-	-
M112	97.167	+2H,+OH	287.0943	287.0925	$C_{16}H_{16}O_5$	6.27	9	269.0794;254.0596;163.0388; 151.0451;145.0348;137.0334; 134.0482;125.0180;123.0592	0.06%	-	-	0.74%	-	-	-	-	-	-	-	-	-
M113	120.348	+2H,+OH	287.0922	287.0925	$C_{16}H_{16}O_5$	-1.04	9	269.0853;254.0584;137.0195	-	-	-	-	-	1.62%	-	-	-	-	-	-	-
M114[a]	99.483	+2H,+OH,+SO_3	367.0488	367.0493	$C_{16}H_{16}O_8S$	-1.36	9	287.0921;245.0126;229.0108; 177.0598;165.0603;163.0388; 161.0254;151.0417;150.0382; 149.0653;135.0589;137.0213; 122.0312;121.0308	2.41%	-	0.09%	2.60%	1.93%	0.40%	-	-	1.17%	-	-	-	-	-
M115[a]	101.892	+2H,+OH,+SO_3	367.0504	367.0493	$C_{16}H_{16}O_8S$	3.00	9	287.0918;230.9941;177.0590; 165.0631;151.0440;150.0407; 147.0412;139.0448;136.0182 135.0397;135.0088;121.0302	0.37%	-	-	-	-	-	-	-	0.20%	-	-	-	-
M116[a]	104.440	+2H,+OH,+SO_3	367.0488	367.0493	$C_{16}H_{16}O_8S$	-1.36	9	287.0924;255.0659;245.0109; 165.0537;150.0341;149.0587; 135.0369;121.0313	0.52%	-	-	0.65%	-	-	-	-	0.28%	-	-	-	-
M117[a]	105.198	+2H,+OH,+SO_3	367.0504	367.0493	$C_{16}H_{16}O_8S$	3.00	9	287.0919;255.0653;177.0588; 165.0547;162.0314;150.0346; 137.0295;135.0377;121.0255	0.96%	-	-	-	0.85%	-	-	-	-	-	-	-	-

Figure 14. *Cont.*

No.	$t_{R(min)}$	Identification	Meas. mass	Pred. mass	Molecular Formula	Error (ppm)	DBE	MS fragments	urine	feces	plasma	colon	intestine	stomach	liver	spleen	kidney	lung	heart	brain	thymus
M118[a]	107.248	+2H,+OH,+SO_3	367.0526	367.0493	$C_{16}H_{16}O_8S$	8.99	9	287.0890;269.0794;151.0382; 149.0629;121.0406	0.30%	-	-	-	-	-	-	-	-	-	-	-	-
M119[a]	110.102	+2H,+OH,+SO_3	367.0493	367.0493	$C_{16}H_{16}O_8S$	0.00	9	287.0920;269.0812;254.0603; 229.0197;177.0583;149.0648; 137.0327;135.0479;134.0647	1.52%	-	1.95%	-	0.20%	1.06%	-	-	1.08%	-	-	-	-
M120[a]	125.240	+2H,+OH,+SO_3	367.0529	367.0493	$C_{16}H_{16}O_8S$	9.81	9	287.0935;255.0683;215.0016; 165.0559;151.0417;150.0322; 137.0207;135.0476	0.50%	2.85%	-	-	-	-	-	-	-	-	-	-	-
M121	61.957	+2H,+OH,+GlcUA	463.1239	463.1246	$C_{22}H_{24}O_{11}$	-1.51	11	175.0289	-	-	-	-	0.18%	-	-	-	-	-	-	-	-
M122	63.735	+2H,+OH,+GlcUA	463.1240	463.1246	$C_{22}H_{24}O_{11}$	-1.30	11	287.0955	-	-	-	-	0.12%	-	-	-	-	-	-	-	-
M123	66.483	+2H,+OH,+GlcUA	463.1274	463.1246	$C_{22}H_{24}O_{11}$	6.05	11	287.0915;272.0633;175.0243	0.32%	-	-	-	0.85%	-	-	-	0.17%	-	-	-	-
M124	69.075	+2H,+OH,+GlcUA	463.1270	463.1246	$C_{22}H_{24}O_{11}$	5.18	11	445.1128;287.0818;269.0797; 254.0519;175.0287	0.24%	-	-	-	0.09%	-	-	-	-	-	-	-	-
M125	69.567	+2H,+OH,+GlcUA	463.1264	463.1246	$C_{22}H_{24}O_{11}$	3.89	11	287.0872;269.0771;254.0696; 175.0232	0.28%	-	-	-	0.20%	-	-	-	0.06%	-	-	-	-
M126	71.158	+2H,+OH,+GlcUA	463.1271	463.1246	$C_{22}H_{24}O_{11}$	5.40	11	287.0898;272.0654	0.24%	-	-	-	0.32%	-	-	-	-	-	-	-	-
M127	74.375	+2H,+OH,+GlcUA	463.1247	463.1246	$C_{22}H_{24}O_{11}$	0.22	11	287.0746	0.09%	-	-	-	-	-	-	-	-	-	-	-	-
M128	82.950	+2H,+OH,+GlcUA	463.1258	463.1246	$C_{22}H_{24}O_{11}$	2.59	11	287.0913;269.0843;254.0639; 175.0230	0.40%	-	-	-	0.41%	-	-	-	0.12%	-	-	-	-
M129	84.275	+2H,+OH,+GlcUA	463.1244	463.1246	$C_{22}H_{24}O_{11}$	-0.43	11	287.0896;163.0509;151.0301; 145.0269	0.06%	-	-	-	0.05%	-	-	-	-	-	-	-	-
M130	85.670	+2H,+OH,+GlcUA	463.1202	463.1246	$C_{22}H_{24}O_{11}$	-9.50	11	287.0874;269.0830;255.0558; 254.0580;137.0150	-	-	-	-	0.20%	-	-	-	-	-	-	-	-
M131	94.032	+2H,+OH,+GlcUA	463.1235	463.1246	$C_{22}H_{24}O_{11}$	-2.38	11	287.0899;269.0927;175.0233; 254.0607;151.0332	-	-	-	-	0.55%	-	-	-	-	-	-	-	-
M132	77.583	+2H,+OH,+2GlcUA	639.1620	639.1567	$C_{28}H_{32}O_{17}$	8.29	13	463.1251;287.0919	0.08%	-	-	-	-	-	-	-	-	-	-	-	-
M133	112.893	+2H,+OH,+CH_3	301.1098	301.1081	$C_{17}H_{18}O_5$	5.65	9	286.0989	0.03%	-	-	-	0.02%	-	-	-	-	-	-	-	-
M134	89.058	+2H,+OH,+CH_3,+GlcUA	477.1370	477.1402	$C_{23}H_{26}O_{11}$	-6.71	11	301.1037;286.0797	0.05%	-	-	-	0.45%	-	-	-	-	-	-	-	-
M135	90.842	+2H,+OH,+CH_3,+GlcUA	477.1438	477.1402	$C_{23}H_{26}O_{11}$	7.54	11	301.1044;286.0796;175.0366	0.77%	-	0.11%	-	2.28%	0.26%	0.83%	-	0.70%	-	-	-	-
M136	91.367	+2H,+OH,+CH_3,+GlcUA	477.1411	477.1402	$C_{23}H_{26}O_{11}$	1.89	11	301.1085;286.0858	0.19%	-	-	-	0.31%	-	-	-	-	-	-	-	-
M137[a]	115.198	+2H,+OH,+CH_3,+SO_3,+GlcUA	557.0988	557.0970	$C_{23}H_{26}O_{14}S$	3.23	11	381.0615;301.1049;286.0779	0.12%	-	-	-	-	-	-	-	-	-	-	-	-
M138	91.925	+2H,+OH,+Vc	445.1170	445.1140	$C_{22}H_{22}O_{10}$	6.74	12	287.0919;161.0254	-	0.37%	-	-	-	-	-	-	-	-	-	-	-
M139	70.173	-CH_3,+2H,+OH	273.0742	273.0768	$C_{15}H_{14}O_5$	-9.52	9	149.0567	-	-	-	0.38%	-	-	-	-	-	-	-	-	-
M140	73.442	-CH_3,+2H,+OH,+SO_3	353.0341	353.0337	$C_{15}H_{14}O_8S$	1.13	9	273.0713;200.9897;161.0303; 151.0448;149.0278;137.0308; 123.0390;121.0329	0.22%	-	-	0.21%	-	-	-	-	-	-	-	-	-
M141	75.225	-CH_3,+2H,+OH,+SO_3	353.0317	353.0337	$C_{15}H_{14}O_8S$	-5.67	9	273.0766;255.0651;163.0509; 137.0263	0.04%	-	-	-	-	-	-	-	-	-	-	-	-
M142	77.075	-CH_3,+2H,+OH,+SO_3	353.0326	353.0337	$C_{15}H_{14}O_8S$	-3.12	9	273.0713;255.0656	0.05%	-	-	-	-	-	-	-	-	-	-	-	-
M143	88.267	-CH_3,+2H,+OH,+SO_3	353.0332	353.0337	$C_{15}H_{14}O_8S$	-1.42	9	335.0202;255.0632;	0.14%	-	-	-	-	-	-	-	-	-	-	-	-
M144[a]	100.758	-CH_3,+2H,+OH,+SO_3	353.0328	353.0337	$C_{15}H_{14}O_8S$	-2.55	9	273.0782;163.0437;161.0315; 151.0428;147.0451;121.0276	0.81%	-	-	1.94%	0.27%	-	-	-	0.24%	-	-	-	-
M145	102.548	-CH_3,+2H,+OH,+SO_3	353.0341	353.0337	$C_{15}H_{14}O_8S$	1.13	9	273.0755;255.0644;163.0457; 149.0673;145.0269;137.0273	0.72%	1.04%	-	2.89%	0.18%	-	-	-	-	-	-	-	-

Figure 14. *Cont.*

No.	$t_{R(min)}$	Identification	Meas. mass	Pred. mass	Molecular Formula	Error (ppm)	DBE	MS fragments	urine	feces	plasma	colon	intestine	stomach	liver	spleen	kidney	lung	heart	brain	thymus
M146	82.908	-CH_3,+2H,+OH,+SO_3	353.0339	353.0337	$C_{15}H_{14}O_8S$	0.57	9	273.0557;216.9794;137.0325	-	0.82%	-	-	-	-	-	-	-	-	-	-	-
M147	57.275	-CH_3,+2H,+OH,+GlcUA	449.1109	449.1089	$C_{21}H_{22}O_{11}$	4.45	11	273.0846;175.0240	0.10%	-	-	-	0.04%	-	-	-	-	-	-	-	-
M148	71.217	-CH_3,+2H,+OH,+GlcUA	449.1098	449.1089	$C_{21}H_{22}O_{11}$	2.00	11	273.0726;175.0249;151.0311	0.21%	-	-	-	0.28%	-	-	-	-	-	-	-	-
M149	61.592	-CH_3,+2H,+OH,+GlcUA	449.1070	449.1089	$C_{21}H_{22}O_{11}$	-4.23	11	273.0847;255.0496	-	-	-	-	0.05%	-	-	-	-	-	-	-	-
M150	58.475	-CH_3,+2OH,+GlcUA	463.0903	463.0882	$C_{21}H_{20}O_{10}$	4.53	12	287.0606;255.0280	-	-	0.22%	-	-	-	-	-	-	-	-	-	-
M151	60.595	-CH_3,+2OH,+GlcUA	463.0891	463.0882	$C_{21}H_{20}O_{10}$	1.94	12	287.0552;255.0278	-	-	0.23%	-	-	-	-	-	-	-	-	-	-
M152[a]	75.058	-CH_3,+2OH,+SO_3	367.0121	367.0129	$C_{15}H_{12}O_9S$	-2.18	10	287.0646;269.0493;177.0282	0.03%	-	-	-	-	-	-	-	-	-	-	-	-
M153[a]	77.742	-CH_3,+2OH,+SO_3	367.0118	367.0129	$C_{15}H_{12}O_9S$	3.00	10	287.0577;177.0333;161.0182; 125.0338;121.0302	0.10%	-	-	-	-	-	-	-	-	-	-	-	-
M154[a]	82.558	-CH_3,+2OH,+SO_3	367.0173	367.0129	$C_{15}H_{12}O_9S$	11.99	10	287.0552;161.0262	0.05%	-	-	-	-	-	-	-	-	-	-	-	-
M155[a]	94.808	-CH_3,+2OH,+SO_3	367.0152	367.0129	$C_{15}H_{12}O_9S$	6.27	10	287.0545;269.0456;163.0339; 137.0363	0.15%	-	-	-	-	-	-	-	-	-	-	-	-
M156[a]	125.455	-CH_3,+2OH,+SO_3	367.0160	367.0129	$C_{15}H_{12}O_9S$	8.45	10	287.0603;255.0270	-	-	0.79%	-	-	-	-	-	-	-	-	-	-
M157[a]	113.177	+2OH,+SO_3	381.0280	381.0286	$C_{16}H_{14}O_9S$	-1.57	10	301.0799;286.0481	0.05%	-	-	-	-	-	-	-	-	-	-	-	-
M158[a]	125.972	+2OH,+SO_3	381.0291	381.0286	$C_{16}H_{14}O_9S$	1.31	10	301.0717;286.0474;161.0298	1.69%	-	-	-	-	-	-	-	0.96%	-	-	-	-
M159[a]	129.862	+2OH,+SO_3	381.0292	381.0286	$C_{16}H_{14}O_9S$	1.57	10	366.0054;301.0711;286.0477; 203.9750;161.0269;149.0301; 137.0229;133.0328;124.0254; 123.0137	12.68%	-	-	-	-	-	-	-	3.71%	-	-	-	-
M160[a]	81.683	+2OH,+SO_3,+GlcUA	557.0652	557.0607	$C_{22}H_{22}O_{15}S$	8.08	12	381.0249;301.0767;286.0504	0.05%	-	-	-	-	-	-	-	-	-	-	-	-
M161[a]	100.708	+2OH,+SO_3,+GlcUA	557.0617	557.0607	$C_{22}H_{22}O_{15}S$	1.80	12	477.1039;381.0247;301.0708; 286.0460	0.12%	-	-	-	-	-	-	-	-	-	-	-	-
M162	67.688	+2H,+2OH	303.0861	303.0874	$C_{16}H_{16}O_6$	-4.29	9	285.0759;273.0731;270.0590	-	-	-	1.92%	-	-	-	-	-	-	-	-	-
M163[a]	56.167	+2H,+3OH,+SO_3	399.0412	399.0391	$C_{16}H_{16}O_{10}S$	5.26	9	381.0296;301.0664;286.0504	0.03%	-	-	-	-	-	-	-	-	-	-	-	-
M164[a]	99.317	+2H,+3OH,+CH_3,+SO_3	413.0521	413.0548	$C_{17}H_{18}O_{10}S$	-6.54	9	381.0275;301.0671;286.0517	0.06%	-	-	-	-	-	-	-	-	-	-	-	-
M165[a]	58.817	-CH_3,+2H,+2OH,+SO_3	369.0297	369.0286	$C_{15}H_{14}O_9S$	2.98	9	351.0135;271.0607	0.07%	-	-	-	-	-	-	-	-	-	-	-	-
Total detected metabolites in the matrix									104	29	38	41	74	28	24	15	42	8	10	3	17

Figure 14. The distribution of 165 metabolites of medicarpin and their relative contents in 13 biosamples ([a], new compounds). The relative content of a metabolite in each biosample was calculated by (peak area of a metabolite/total peak area of all detected metabolites) × 100%.

Table 1. Relative contents of metabolic reactions and phase I metabolites of medicarpin in 13 biological samples (%).

Biosample	Relative Contents (%)								
	Phase I Reaction			Phase II Reaction					Phase I Metabolites
	-CH_3	+2H	+OH	+SO_3	+GlcUA	+Vc	+Glc	+CH_3	
urine	55.14	37.01	57.79	74.60	25.83	1.08	0.23	3.93	1.78
feces	71.51	44.43	21.55	73.53	1.62	15.54	—	— [1]	9.30
plasma	36.58	25.72	22.78	36.17	67.87	0.44	—	3.16	—
colon	57.95	58.48	28.30	55.81	16.61	9.23	—	0.78	17.57
intestine	39.56	41.46	36.17	15.62	78.04	7.60	—	11.23	0.99
stomach	39.46	22.38	26.67	35.00	54.57	1.23	—	2.50	9.20
liver	62.62	31.43	13.33	57.11	42.09	—	—	3.55	0.80
spleen	33.84	23.45	8.74	27.79	71.33	—	—	1.03	0.88
kidney	60.90	30.46	34.93	63.43	36.30	0.10	—	1.67	0.17
lung	34.25	22.91	5.29	28.22	71.78	—	—	—	—
heart	33.74	22.74	6.19	27.76	71.70	—	—	—	0.54
brain	57.11	20.86	—	57.11	42.89	—	—	—	—
thymus	25.25	15.66	9.12	18.96	80.54	—	—	2.01	0.49

[1] —, undetected.

3. Materials and Methods

3.1. Chemicals and Reagents

Medicarpin (Molecular formula: $C_{16}H_{14}O_4$, exact mass: 270.0892 Da) was isolated from the Maackia amurensis Radix by chromatographic methods, including 200–300 mesh normal phase silica gel (Sinopharm Chemical Reagent Co., Ltd., Shanghai, China) column chromatography and reversed phase C18 silica gel (YMC, YMC Co., Ltd., Kyoto, Japan) column chromatography. The optical rotation angle was $[\alpha]_{25}^{L}$ = −19.92 (c = 5, CH_3OH). Hence, its structure was determined to be (−)-3-hydroxy-9-methoxypterocarpan or (−)-medicarpin on the basis of UV, NMR, and MS data. Its purity was greater than 98% by the peak area normalization method using HPLC-UV analysis at 280 nm. Formic acid (Fisher scientific, Fair lawn, NJ, USA), acetonitrile (Fisher scientific), and methanol (Tianjin Damao Chemicals, Tianjin, China) were of HPLC grade. Ultrapure water was prepared using a Milli-Q water purification system (Millipore, Billerica, MA, USA). Analytical grade sodium carboxymethyl cellulose (CMC-Na) was purchased from Tianjin Guangfu Fine Chemical Research Institute (Tianjin, China). All other chemicals and reagents were of analytical grade.

3.2. Animals and Drug Administration

Eight male Sprague-Dawley rats (220–250 g) were obtained from the Experimental center of Peking University Health Science Center (Beijing, China). All rats were housed in a controlled animal room. Before oral gavage, the rats were randomly divided into two groups (a drug group and a blank group, four rats per group). Each rat was housed in a metabolic cage with water and food ad libitum for three days. Medicarpin was suspended in 0.5% CMC-Na solution and administrated at a dose of 100 mg/kg (body weight) to the drug group rats once a day for four days, while the blank group were given the same volume of 0.5% CMC-Na. All animal treatments were approved by the Biomedical Ethical Committee of Peking University (approval No. LA2015134).

3.3. Sample Collection and Preparation

Urine and feces samples were collected for the first three days after drug administration; plasma samples and organ samples were collected on the last day one hour after drug administration.

Urine samples: All urine samples from the same group were merged and evaporated to dryness at 40 °C using a Laborota 4001 rotator evaporator (Heidolph Instruments GmbH & Co., Schwabach, Germany) under vacuum, respectively. Then, each group added 10 volumes of methanol (10 mL methanol/g residue) and extracted ultrasonically for 30 min. The extracts were filtered and evaporated

to dryness at 40 °C. Finally, the residues were dissolved in 2 volumes of methanol (2 mL methanol/g residue), filtered through 0.22 μm membranes, and stored at −80 °C before further analysis.

Feces samples: All feces samples from the same group were dried at 50 °C and crushed into powder, respectively. Then, each group was ultrasonically extracted with 10 volumes (mL/g) of methanol for 30 min and filtered, after that the filtrate was evaporated to dryness at 40 °C. The residues were dissolved in 4 volumes of methanol (4 mL methanol/g residue), filtered through 0.22 μm membranes before being stored at −80 °C.

Plasma samples: An hour after the last drug administration, the blood was collected in heparin tubes by cardiac puncture technique in groups through anesthetizing with an intraperitoneal injection of chloral hydrate. Plasma was obtained after centrifugation at 2292× *g* (5000 rpm), 4 °C for 15 min using a 3–30 K refrigerated centrifuge (Sigma Laborzentrifugen GmbH, Osterode am Harz Germany). Afterwards, each plasma sample was ultrasonically extracted with 10 volumes (mL/mL) of methanol for 30 min in order to remove the protein content and then centrifuged for 15 min at 2292× *g* (5000 rpm), 4 °C. The supernatant of each group was evaporated to dryness under vacuum by a rotator evaporator. Then the residue was dissolved in 1 volume of methanol (1 mL methanol/g residue) and filtered through 0.22 μm membranes before stored at −80 °C.

Organ samples: After collecting blood via cardiac puncture, the heart, liver, spleen, lungs, kidneys, colon, intestine, stomach, brain, thymus were rapidly removed and washed three times with cold saline to flush away the surface blood and other residual substances. Later, they were preserved at −80 °C after drying with filter papers. Then, each kind of the organs from the same group were combined and weighed, as well as added 5 times volumes of methanol (5 mL methanol/g tissue). The mixture was homogenized by a T10 homogenizer (IKA Co., Ltd., Staufen, Germany) under low temperature conditions, and ultrasonically extracted by a KQ-2200B ultrasonic cleaning machine (Kunshan Ultrasonic Instruments Co., Ltd., Jiangsu, China) for an hour and then centrifuged at 2292× *g* (5000 rpm) at 4 °C for 15 min. Additionally, the supernatant was concentrated and dried in a vacuum at 40 °C, reconstituted with 10 times volume of methanol, and maintained at −80 °C. And, before LC-MS analysis they shall be filtered through 0.22 μm membranes.

3.4. Instrumentation and Analytical Conditions

The chromatographic separation was performed on the Agilent HPLC instrument using a Phenomenex Gemini C18 column (250 mm × 4.60 mm, 5 μm). The column oven temperature was maintained at 35 °C and the volume injected was 10 μL. The mobile phases were water (contained 0.1% formic acid, *v*/*v*) (A) and acetonitrile (B). The gradient elution program was as follows: 0–10 min, 3% B; 10–130 min, 3–40% B; 130–140 min, 40–100% B; 140–155 min, 100% B. The flow rate was 1.0000 mL/min.

HPLC-ESI-IT-TOF-MS^n analysis was performed on a Shimadzu LC-MS-IT-TOF instrument, which consists of a CBM-20A system controller, two LC-20AD pumps, an SIL-20AC autosampler, a CTO-20A column oven, an SPD-M20A PDA detector, an ESI ion source, and an IT-TOF mass spectrometer using the same separation conditions. The mass spectrometer flow rate was 0.2000 mL/min that was split from HPLC effluent and the detection mode included positive ion (ESI+) and negative ion (ESI−) mode with a full-scan covering *m*/*z* 100–1000 (MS) and *m*/*z* 50–1000 (MS^2 and MS^3). The other optimal conditions were set as follows: heat block and curved desolvation line temperature was 250 °C and nebulizing nitrogen gas flow was 1.5 mL/min; the interface voltage was (+)-4.5 kV and (−)-5.5 kV and the detector voltage was 1.7 kV. In addition, the ion accumulation time was 30 ms and the relative collision-induced dissociation energy was 70%. The mass range *m*/*z* 50–3000 was calibrated by a trifluoroacetic acid sodium solution (2.5 mM). All data were acquired and analyzed by Shimadzu LCMS solution Version 3.60, Formula Predictor Version 1.2, and Accurate Mass Calculator (Shimadzu, Kyoto, Japan).

4. Conclusions

In this paper, the metabolites of medicarpin and their distributions in rats were systematically studied for the first time, and 165 new metabolites (13 phase I metabolites and 152 phase II metabolites) were tentatively identified by HPLC-ESI-IT-TOF-MS^n, including 104 metabolites in urine, 29 in feces, 38 in plasma, 41 in the colon, 74 in the intestine, 28 in the stomach, 24 in the liver, 15 in the spleen, 42 in the kidney, eight in the lung, 10 in the heart, three in the brain and 17 in the thymus. Eighty-six sulfate metabolites, five Vitamin C conjugates (**M3**, **M8**, **M9**, **M24**, **M25**) and two hydroxylated medicarpin glucuronides (**M5** and **M6**) were regarded as potential new compounds by retrieving information from the Scifinder database. Besides, based on the structure of these metabolites, the metabolic pathways of medicarpin were proposed. The metabolic reactions of medicarpin included demethylation, hydrogenation, hydroxylation, glucuronidation, sulfation, glycosylation, methylation and conjunction of vitamin C, among which sulfation and glucuronidation were the major phase II metabolic reactions. Five metabolites (**M1**, **M5**, **M30**, **M12**, **M27**) were widely distributed to nine or ten organs, and the specific distribution of lots of metabolites (e.g., **M2**, **M14**, **M20**, **M35**, **M40**, **M54**, **M109**) were also discovered. Furthermore, we found that isomerization of medicarpin must occur in vivo. This study is the first comprehensive report on the metabolism of pterocarpans in animals. The results will facilitate the understanding of the metabolism of medicarpin, and will provide a scientific basis for further pharmacological studies on medicarpin and for metabolism research of other pterocarpans in animals.

Supplementary Materials: Figures S1–S52 are available online.

Author Contributions: Conceptualization, F.X.; methodology, F.X.; validation, F.X., T.L.; formal analysis, H.-Y.W.; investigation, H.-Y.W., T.L., R.J.; writing—original draft preparation, H.-Y.W.; writing—review and editing, H.-Y.W., F.X., M.-Y.S., G.-X.L., Y.-L.L., S.-Q.C.; supervision, F.X., M.-Y.S.; project administration, F.X.; funding acquisition, F.X.

Funding: This study was financially supported by the National Natural Science Foundation of China (No. 81573593).

Conflicts of Interest: The authors declare no conflict of interest.

References

1. Harper, S.H.; Kemp, A.D.; Underwood, W.G.E. Heartwood constituents of *Stoarfzia madagascariensis*. *Chem. Comm.* **1965**, *14*, 309–310.
2. Belofsky, G.; Kolaczkowski, M.; Adams, E.; Schreiber, J.; Eisenberg, V.; Coleman, C.M.; Zou, Y.; Ferreira, D. Fungal ABC tansporter-associated activity of isoflavonoids from the root extract of *Dalea formosa*. *J. Nat. Prod.* **2013**, *76*, 915–925. [CrossRef]
3. Rukachaisirikul, T.; Innok, P.; Aroonrerk, N.; Boonamnuaylap, W.; Limrangsun, S.; Boonyon, C.; Woonjina, U.; Suksamrarn, A. Antibacterial pterocarpans from *Erythrina subumbrans*. *J. Ethnopharmacol.* **2007**, *110*, 171–175. [CrossRef]
4. Weng, J.; Tsao, L.; Yen, M.; Wang, J.; Lin, C. Anti-inflammatory constituents and new pterocarpanoid of *Crotalaria pallida*. *J. Nat. Prod.* **2003**, *66*, 404–407. [CrossRef]
5. Zhou, H.; Lutterodt, H.; Cheng, Z.; Yu, L.L. Anti-inflammatory and antiproliferative activities of trifolirhizin, a flavonoid from *Sophora flavescens* Roots. *J. Agric. Food Chem.* **2009**, *57*, 4580–4585. [CrossRef]
6. Zhang, L.; Liu, H.; Hsiao, P.; Kuo, L.Y.; Lee, I.; Wu, T.; Chiou, W.; Kuo, Y. New isoflavonoid glycosides and related constituents from Astragali Radix (*Astragalus membranaceus*) and their inhibitory activity on nitric oxide production. *J. Agric. Food Chem.* **2011**, *59*, 1131–1137. [CrossRef]
7. Kuete, V.; Sandjo, L.P.; Djeussi, D.E.; Zeino, M.; Kwamou, G.M.N.; Ngadjui, B.; Efferth, T. Cytotoxic flavonoids and isoflavonoids from *Erythrina sigmoidea* towards multi-factorial drug resistant cancer cells. *Invest. New Drugs* **2014**, *32*, 1053–1062. [CrossRef]
8. Mahajan, P.; Gnana, O.R.; Jachak, S.M.; Bharate, S.B.; Chaudhuri, B. Antioxidant and antiproliferative activity of indigocarpan, a pterocarpan from *Indigofera aspalathoides*. *J. Pharm. Pharmacol.* **2016**, *68*, 1331–1339. [CrossRef]

9. Nguyen, P.H.; Le, T.V.T.; Thuong, P.T.; Dao, T.T.; Ndinteh, D.T.; Mbafor, J.T.; Kang, K.W.; Oh, W.K. Cytotoxic and PTP1B inhibitory activities from *Erythrina abyssinica*. *Bioorg. Med. Chem. Lett.* **2009**, *19*, 6745–6749. [CrossRef]
10. Bhargavan, B.; Singh, D.; Gautam, A.K.; Mishra, J.S.; Kumar, A.; Goel, A.; Dixit, M.; Pandey, R.; Manickavasagam, L.; Dwivedi, S.D.; et al. Medicarpin, a legume phytoalexin, stimulates osteoblast differentiation and promotes peak bone mass achievement in rats: Evidence for estrogen receptor β-mediated osteogenic action of medicarpin. *J. Nutr. Biochem.* **2012**, *23*, 27–38. [CrossRef]
11. Kureel, J.; Dixit, M.; Tyagi, A.M.; Mansoori, M.N.; Srivastava, K.; Raghuvanshi, A.; Maurya, R.; Trivedi, R.; Goel, A.; Singh, D. miR-542-3p suppresses osteoblast cell proliferation and differentiation, targets BMP-7 signaling and inhibits bone formation. *Cell Death Dis.* **2014**, *5*, e1050. [CrossRef]
12. Tyagi, A.M.; Gautam, A.K.; Kumar, A.; Srivastava, K.; Bhargavan, B.; Trivedi, R.; Saravanan, S.; Yadav, D.K.; Singh, N.; Pollet, C.; et al. Medicarpin inhibits osteoclastogenesis and has nonestrogenic bone conserving effect in ovariectomized mice. *Mol. Cell Endocrinol.* **2010**, *325*, 101–109. [CrossRef]
13. Vieira, N.C.; Espíndola, L.S.; Santana, J.M.; Veras, M.L.; Pessoa, O.D.; Pinheiro, S.M.; de Araujo, R.M.; Lima, M.A.; Silveira, E.R. Trypanocidal activity of a new pterocarpan and other secondary metabolites of plants from Northeastern Brazil flora. *Bioorg. Med. Chem.* **2008**, *16*, 1676–1682. [CrossRef]
14. Rosa, A.; Deiana, M.; Corona, G.; Atzeri, A.; Incani, A.; Appendino, G.; Dessì, M.A. Antioxidant properties of extracts and compounds from *Psoralea morisiana*. *Eur. J. Lipid Sci. Technol.* **2005**, *107*, 521–529. [CrossRef]
15. Fotso, G.W.; Maher, F.A.; Ngnintedo, D.; Ango, P.Y.; Kapche, D.G.F.W.; Ngameni, B.; Ngwenya, B.; Yeboah, S.O.; Ngadjui, B.T.; Andrae-Marobela, K. Three new isoflavonoids with antioxidant properties from *Ptycholobium contortum* (N.E.Br.) Brummitt (Leguminosae). *Phytochem. Lett.* **2015**, *14*, 254–259. [CrossRef]
16. Selvam, C.; Jachak, S.M.; Gnana Oli, R.; Thilagavathi, R.; Chakraborti, A.K.; Bhutani, K.K. A new cyclooxygenase (COX) inhibitory pterocarpan from *Indigofera aspalathoides*: Structure elucidation and determination of binding orientations in the active sites of the enzyme by molecular docking. *Tetrahedron Lett.* **2004**, *45*, 4311–4314. [CrossRef]
17. Yuk, H.J.; Curtis-Long, M.J.; Ryu, H.W.; Jang, K.C.; Seo, W.D.; Kim, J.Y.; Kang, K.Y.; Park, K.H. Pterocarpan profiles for soybean leaves at different growth stages and investigation of their glycosidase inhibitions. *J. Agric. Food Chem.* **2011**, *59*, 12683–12690. [CrossRef]
18. Ryu, Y.B.; Curtis-Long, M.J.; Kim, J.H.; Jeong, S.H.; Yang, M.S.; Lee, K.W.; Lee, W.S.; Park, K.H. Pterocarpans and flavanones from *Sophora flavescens* displaying potent neuraminidase inhibition. *Bioorg. Med. Chem. Lett.* **2008**, *18*, 6046–6049. [CrossRef]
19. Woo, H.S.; Kim, D.W.; Curtis-Long, M.J.; Lee, B.W.; Lee, J.H.; Kim, J.Y.; Kang, J.E.; Park, K.H. Potent inhibition of bacterial neuraminidase activity by pterocarpans isolated from the roots of *Lespedeza bicolor*. *Bioorg. Med. Chem. Lett.* **2011**, *21*, 6100–6103. [CrossRef]
20. Mori-Hongo, M.; Takimoto, H.; Katagiri, T.; Kimura, M.; Ikeda, Y.; Miyase, T. Melanin synthesis inhibitors from *Lespedeza floribunda*. *J. Nat. Prod.* **2009**, *72*, 194–203. [CrossRef]
21. Boué, S.M.; Burow, M.E.; Wiese, T.E.; Shih, B.Y.; Elliott, S.; Carter-Wientjes, C.H.; McLachlan, J.A.; Bhatnagar, D. Estrogenic and antiestrogenic activities of phytoalexins from red kidney bean (*Phaseolus vulgaris* L.). *J. Agric. Food. Chem.* **2011**, *59*, 112–120. [CrossRef]
22. Maurich, T.; Pistelli, L.; Turchi, G. Anti-clastogenic activity of two structurally related pterocarpans purified from *Bituminaria bituminosa* in cultured human lymphocytes. *Mutat. Res.* **2004**, *561*, 75–81. [CrossRef] [PubMed]
23. Zhang, W.; Xu, F.; Wang, D.; Ye, J.; Cai, Q. Buyang Huanwu Decoction ameliorates ischemic stroke by modulating multiple targets with multiple components: In vitro evidences. *Chin. J. Nat. Med.* **2018**, *16*, 0194–0202. [CrossRef]
24. Ahmad, V.U.; Iqbal, S.; Nawaz, S.A.; Choudhary, M.I.; Farooq, U.; Ali, S.T.; Ahmad, A.; Bader, S.; Kousar, F.; Arshad, S.; et al. Isolation of four new pterocarpans from *Zygophyllum eurypterum* (Syn. *Z. atriplicoides*) with enzyme-inhibition properties. *Chem. Biodivers.* **2006**, *3*, 996–1003. [CrossRef] [PubMed]
25. Chen, L.; Liu, Y.; Zhang, H.; Liang, S. In-vivo study of metabolism of trifolirhizin in rats. *Trad. Chin. Drug Res. Clin. Pharmacol.* **2012**, *23*, 174–177.
26. Hargreaves, J.A.; Mansfield, J.W.; Coxon, D.T. Identification of medicarpin as a phytoalexin in the broad bean plant (*Vicia Jaba* L.). *Nature* **1976**, *262*, 318–319. [CrossRef]

27. Kim, J.M.; Lee, Y.M.; Lee, G.Y.; Jang, D.S.; Bae, K.H.; Kim, J.S. Constituents of the roots of *Pueraria lobata* inhibit formation of advanced glycation end products (AGEs). *Arch. Pharm. Res.* **2006**, *29*, 821–825. [CrossRef]
28. Liu, Y.; Chen, H.; Zhao, Y.; Wang, B.; Zhang, Q.; Zhang, L.; Tu, P. Quantification and stability studies on the flavonoids of Radix hedysari. *J. Agric. Food Chem.* **2006**, *54*, 6634–6639. [CrossRef]
29. Rayanil, K.; Bunchornmaspan, P.; Tuntiwachwuttikul, P. A new phenolic compound with anticancer activity from the wood of *Millettia leucantha*. *Arch. Pharm. Res.* **2011**, *34*, 881–886. [CrossRef]
30. Gatouillat, G.; Magid, A.A.; Bertin, E.; El Btaouri, H.; Morjani, H.; Lavaud, C.; Madoulet, C. Medicarpin and millepurpan, two flavonoids isolated from *Medicago sativa*, induce apoptosis and overcome multidrug resistance in leukemia P388 cells. *Phytomedicine* **2015**, *22*, 1186–1194. [CrossRef] [PubMed]
31. Martínez-Sotres, C.; López-Albarrán, P.; Cruz-de-León, J.; García-Moreno, T.; Rutiaga-Quiñones, J.G.; Vázquez-Marrufo, G.; Tamariz-Mascarúa, J.; Herrera-Bucio, R. Medicarpin, an antifungal compound identified in hexane extract of *Dalbergia congestiflora* Pittier heartwood. *Int. Biodeterior. Biodegrad.* **2012**, *69*, 38–40. [CrossRef]
32. Promchai, T.; Janhom, P.; Maneerat, W.; Rattanajak, R.; Kamchonwongpaisan, S.; Pyne, S.G.; Limtharakul, T. Antibacterial and cytotoxic activities of phenolic constituents from the stem extracts of *Spatholobus parviflorus*. *Nat. Prod. Res.* **2018**, 1–5. [CrossRef]
33. Imran, K.M.; Yoon, D.; Kim, Y. A pivotal role of AMPK signaling in medicarpin-mediated formation of brown and beige. *BioFactors* **2018**, *44*, 168–179. [CrossRef]
34. Imran, K.M.; Yoon, D.; Kim, Y.S. Medicarpin induces lipolysis via activation of protein kinase A in brown adipocytes. *BMB Rep.* **2018**, *51*, 249–254. [CrossRef]
35. Ma, L.; Xu, F.; Li, F.; Wang, J.; Shang, M.; Liu, G.; Cai, S. The profiling and identification of the metabolites of 8-prenylkaempferol and a study on their distribution in rats by high-performance liquid chromatography with diode array detection combined with electrospray ionization ion trap time-of-flight multista. *Biomed. Chromatogr.* **2016**, *30*, 175–190. [CrossRef]

Sample Availability: Not available.